JPET Fast Forward. Published on May 22, 2017 as DOI: 10.1124/jpet.117.241117
This article has not been copyedited and formatted. The final version may differ from this version.

TRV0109101, a G protein-biased agonist of the μ-opioid receptor, does not promote opioid-induced mechanical allodynia following chronic administration

Michael Koblish, Richard Carr III, Edward R. Siuda, David H. Rominger, William Gowen-MacDonald, Conrad L. Cowan, Aimee L. Crombie, Jonathan D. Violin, Michael W. Lark

Trevena, Inc., 1018 West 8th Ave., Suite A, King of Prussia, PA 19406 (MK, RC, ERS, DHR, WGM, CLC, ALC, JDV, MWL)

Running title: A G protein-biased MOPR agonist does not promote OIH

To whom correspondence should be addressed: Michael W Lark, PhD. Trevena Inc., 1018 West 8th Ave., Suite A, King of Prussia, PA 19406. E-mail: mlark@trevena.com, website: www.trevena.com, phone number: (610) 354-8840 x223.

Number of text pages = 34

Number of Figures = 6

Number of references = 46

Words in Abstract = 243

Words in Introduction = 675

Words in Discussion = 1514

Number of Supplemental Figures = 8

Number of Supplemental Tables = 3

Abbreviations: β-arr, β-arrestin; cAMP, 3',5'-cyclic adenosine monophosphate; DAMGO, [D-Ala^2, NMe-Phe^4, Gly-ol^5]-enkephalin; DOPR, delta-opioid peptide receptor; DPDPE, [D-Pen2,5]-enkephalin; GPCR, G protein coupled receptor; GRK, G protein receptor kinase; HEK, human embryonic kidney; IBMX, isobutyl methylxanthine; KO, knockout; KOPR, Kappa-opioid peptide receptor; MOPR, mu-opioid peptide receptor; MPE, maximum possible effect; NOPR, nociceptin peptide receptor; OIH, opioid-induced hyperalgesia; OIMA, opioid-induced mechanical allodynia; PK, pharmacokinetics; SDS-PAGE, sodium dodecyl sulfate polyacrylamide gel electrophoresis; TRPV1, transient receptor potential cation channel subfamily V member 1

Section Assignment: Behavioral Pharmacology

JPET Fast Forward. Published on May 22, 2017 as DOI: 10.1124/jpet.117.241117
This article has not been copyedited and formatted. The final version may differ from this version.

ABSTRACT

Prescription opioids are a mainstay in the treatment of acute moderate to severe pain. However, chronic use leads to a host of adverse consequences including tolerance and opioid-induced hyperalgesia (OIH), leading to more complex treatment regimens and diminished patient compliance. Patients experiencing OIH paradoxically experience exaggerated nociceptive responses instead of pain reduction after chronic opioid usage. The development of OIH and tolerance tend to occur simultaneously and, thus, present a challenge when studying the molecular mechanisms driving each phenomenon. We tested the hypothesis that a G protein-biased μ-opioid peptide receptor (MOPR) agonist would not induce symptoms of OIH, such as mechanical allodynia, following chronic administration. We observed that the development of opioid-induced mechanical allodynia (OIMA), a model of OIH, was absent in β-arrestin1$^{-/-}$ and β-arrestin2$^{-/-}$ mice in response to chronic administration of conventional opioids such as morphine, oxycodone and fentanyl, while tolerance developed independent of OIMA. In agreement with the β-arrestin knockout mouse studies, chronic administration of TRV0109101, a G protein-biased MOPR ligand and structural analog of oliceridine, did not promote the development of OIMA but did result in drug tolerance. Interestingly, following induction of OIMA by morphine or fentanyl, TRV0109101 was able to rapidly reverse allodynia. These observations establish a role for β-arrestins in the development of OIH, independent of tolerance, and suggest that the use of G protein-biased MOPR ligands, such as oliceridine and TRV0109101, may be an effective therapeutic avenue for managing chronic pain with reduced propensity for opioid-induced hyperalgesia.

INTRODUCTION

While opioids remain the standard for managing acute moderate to severe pain, their use for treatment of chronic conditions remains controversial (Johannes et al., 2010; Gomes et al., 2014; Trang et al., 2015). In addition to potential for dependence, long-term opioid usage may result in tolerance and opioid-induced hyperalgesia (OIH). With tolerance, opioid dosages need to be increased to maintain the same level of analgesia (Lee et al., 2011; Williams et al., 2013). In contrast, with OIH, increased opioid dose results in a paradoxical increase in pain sensation (Simonnet and Rivat, 2003; Chu et al., 2008; Marion Lee et al., 2011). Individuals with OIH report pain responses from subthreshold stimuli (allodynia) or exaggerated pain in response to noxious stimuli (hyperalgesia). This pain can be diffuse and independent of the original site of injury (Lee et al., 2011). OIH has been observed in response to a variety of μ-opioid peptide receptor (MOPR) agonists including: morphine, oxycodone, fentanyl, remifentanil and even codeine (Seymour et al., 1982; Lipman and Blumenkopf, 1989; Guignard et al., 2000; Angst and Clark, 2006; Chu et al., 2006; Eastman et al., 2014; Johnson et al., 2014; Mauermann et al., 2016). OIH is also prevalent among heroin drug users and those undergoing methadone substitution therapies (Compton et al., 2001; Compton et al., 2012).

The specific molecular mechanisms of OIH are currently unknown. Recent work has highlighted the role of MOPR-mediated signaling on peripheral nociceptors as a primary mechanism in the development of OIH and tolerance (Corder et al., 2017). As regulators and mediators of MOPR signaling, β-arrestins may contribute to this process and have been described with contrasting roles in the development of OIH (Rowan et al., 2014a; Rowan et al., 2014b). In primary sensory neurons, DAMGO and morphine simultaneously recruit β-arrestin to MOPR and decrease β-arrestin interaction with TRPV1 which results in increased sensitivity of TRPV1 (Rowan et al., 2014a; Rowan et al., 2014b). In contrast, DAMGO-mediated mechanical allodynia was prolonged in β-arrestin2 KO mice and attributed to the loss of β-arrestin-mediated

regulation of NMDA receptor function (Chen et al., 2016). β-arrestin2 knockout mice exhibit enhanced and prolonged antinociception to a single dose of morphine (Bohn et al., 1999) and reduced tolerance (Bohn et al., 1999; Bohn et al., 2000; Bohn et al., 2002) while effects on OIH were not documented. As the role of β-arrestins in the development of OIH and tolerance remain ambiguous, we sought to investigate this question further.

Previous work using β-arrestin2 knockout mice has established a role for β-arrestins in other opioid-associated adverse events such as respiratory depression and reduced gastrointestinal function and, thus, supported the rationale for the development of G protein-biased MOPR agonists as differentiated analgesics that promote robust antinociception with reduced liability for adverse events (Bohn et al., 1999; Raehal et al., 2005). G protein-biased MOPR agonists promote more effective coupling to G protein signaling pathways (associated with analgesia) than to β-arrestin recruitment (associated with opioid-induced adverse events) as compared to morphine. Recently characterized G protein-biased MOPR agonists such as oliceridine (TRV130), PZM21 and mitragynine pseudoindoxyl have shown less respiratory depression and gastrointestinal dysfunction than morphine whilst maintaining analgesic efficacy in rodents (DeWire et al., 2013; Manglik et al., 2016; Varadi et al., 2016). Oliceridine has also shown reductions in adverse events in humans (Soergel et al., 2014; Siuda et al., 2016). While mitragynine pseudoindoxyl exhibited delayed antinociceptive tolerance, the effects of biased ligands on OIH have not been reported. Therefore, the use of a G protein-biased MOPR ligand provides a pharmacological approach uniquely positioned to study the contribution of β-arrestins in the development of OIH and opioid-tolerance that may have clinical implications for compounds, like oliceridine, that are in clinical development.

We hypothesized that a G protein-biased MOPR ligand may be able to uncouple the induction of OIH from the development of tolerance. Here, we compare an exemplary G protein-biased MOPR ligand, TRV0109101, to morphine, fentanyl and oxycodone at measures of

opioid-induced mechanical allodynia (OIMA), a model of OIH, and antinociceptive tolerance to assess additional differentiation between G protein-biased MOPR ligands and conventional opioids.

JPET Fast Forward. Published on May 22, 2017 as DOI: 10.1124/jpet.117.241117
This article has not been copyedited and formatted. The final version may differ from this version.

MATERIALS AND METHODS

Chemicals

[D-Ala^2, NMe-Phe^4, Gly-ol^5]-enkephalin (DAMGO, Cat. No. 1171), [D-Pen2,5]-enkephalin (DPDPE, Cat. No. 1431), (-)-U-50488 hydrochloride (Cat. No, 0496), nociceptin (Cat. No. 0910), isobutyl methylxanthine (IBMX, Cat. No. 2845) and NKH 477 (water soluble analog of forskolin, Cat. No. 1603) were purchased from Tocris Bioscience (Ellisville, MO). Morphine Sulfate (Cat. No. M8777), oxycodone HCl (Cat. No. O1378), and fentanyl citrate (Cat. No. F-3886) were purchased from Sigma-Aldrich (St, Louis, MO). Cebranopadol was purchased from MedChem Express (Cat. No.: HY-15536). (R)-TRV0109101 hydrochloride was synthesized at Trevena, Inc. (Chen et al., 2013).

Cell culture

Human embryonic kidney (HEK)-293 cells stably transfected to overexpress β-arrestin-2 fused to a β-galactosidase fragment were purchased from DiscoverX (DiscoverX Corporation, Fremont, CA, Part# 93-0165) and the human OPRM1 gene (NM_000914.3, encoding human μ opioid peptide receptor MOPR), mouse OPRM1 gene (NM_001039652.1, mouse MOPR), human OPRD1 gene [NM_000911.3, human δ-opioid peptide receptor (DOPR)], human OPRK1 gene [NM_000912.3, human κ-opioid peptide receptor (KOPR)], and human OPRL1 gene [NM_182647.2, human nociceptin opioid peptide (NOPR)] receptors were fused to a complementary β-galactosidase fragment using the pCMV-ProLink plasmid purchased from DiscoverX (Part# 93-0167). Cells were grown in minimum Eagle's medium (Corning, 10-010-CM) with 10% fetal bovine serum (Sigma, F2442), 1% penicillin/streptomycin (Corning, 30-002-CL), and 150 μg/ml of G418 sulfate (Corning 30-234-CR) and 150 μg/ml of Hygromycin B (Corning, 0-240-CR).

JPET Fast Forward. Published on May 22, 2017 as DOI: 10.1124/jpet.117.241117
This article has not been copyedited and formatted. The final version may differ from this version.

β-arrestin2 recruitment

Using the stable cell lines described above (MOPR, KOPR, DOPR, NOPR), β-arrestin2 recruitment to each receptor was quantified using the DiscoverX PathHunter β-arrestin recruitment enzyme complementation assay as previously described (DeWire et al., 2013). Briefly, HEK-293 cells stably co-expressing the Prolink-tagged (C-terminus) opioid receptor of interest and β-arrestin2-Prolink acceptor were plated at a density of 5,000 cells per well in white opaque 384-well plates (Greiner Bio One, Part# 784080) and maintained overnight in growth media at 37°C / 5% CO_2. Growth media was removed and test ligand (or vehicle) in assay buffer (Ham's F-12 (Corning, 10-080-CM), 10 mM HEPES (Lonza, 17-737E), 500 μM Isobutyl methylxanthine, and 1.5 μM NKH-477 added. Cells were treated with ligand for 1 hour at 37°C followed by the addition of PathHunter detection reagent (Part# 93-001L). One hour after detection reagent addition β-arrestin2 recruitment was detected by chemiluminescence on a PheraStar plate reader (BMG Labtech, Durham, NC) according to manufacturer's protocol. Ligand potency and efficacy was assessed by concentration-response analysis (idbs, XLfit) and expressed as a normalized percentage of a maximal response.

cAMP accumulation

Using the same cell lines described for β-arrestin2 recruitment, cells were plated and cultured identically to their β-arrestin2 recruitment counterpart. To quantify $G_{\alpha i}$ coupling, the inhibition of forskolin-stimulated cAMP accumulation was detected according to manufacturer's protocol using the cAMP HiRange Kit (Cisbio, Part #62AM6PEJ) after a 30 min incubation with ligand in assay buffer at 37°C / 5% CO_2. After detection reagent addition, plates were incubated for 60 min at room temperature and subsequently read using time-resolved fluorescence (665 nM/620 nM) on a PheraStar plate reader, according to manufacturer's protocol. Ligand potency and

efficacy was assessed by concentration-response analysis (idbs, XLfit) and expressed as a normalized percentage of a maximal response.

Receptor Internalization

The PathHunter GPCR internalization assay (DiscoverX, Part# 93-0745C3) was performed according to the manufacturer's protocol. Receptor localization to the early endosome was detected by chemiluminescence using the PheraStar plate reader, according to manufacturer's instructions.

Agonist-promoted MOPR phosphorylation

HEK293 cells stably expressing human MOPR were cultured in 6-well plates. After an overnight serum starvation, cells were stimulated with 1 μM of morphine, fentanyl, oxycodone or TRV0109101 for 5 min at 37°C. Upon removal of the stimulation media, cells were washed thrice with ice cold PBS and lysed on ice with 20 mM HEPES, 150 mM NaCl, 1% TritonX-100 and 1 CompleteMini protease inhibitor tablet (Roche). Lysates were rocked for 30 min at 4°C and cleared by centrifugation (1000xg for 5 min). Equal protein amounts were separated by SDS-PAGE and transferred to nitrocellulose using an iBlot2 Dry blotting apparatus. Agonist-promoted MOPR phosphorylation was probed by the phospho-specific antibody for MOPR $pSer^{375}$ (Cell Signaling Technology, #3451) as per the manufacturer's instructions and detected using a Syngene G:Box by chemiluminescence. The immunoreactive band representing hMOPR was quantified using LiCOR Image Studio (v5.2) software and reported as normalized values to vehicle-treated cells.

Schild regression analysis

The competitive interaction of TRV0109101 at the human MOPR orthosteric ligand binding site was quantified via Schild analysis using the β-arrestin2 PathHunter human MOPR stable cell

line. Identical culture conditions and assay reagents were used as described in the cAMP accumulation and β-arrestin2 recruitment methods above. Assay protocols were modified at the ligand addition step. After removal of growth media, cells were pretreated with competitor ligand (or vehicle) in assay buffer for 5 min at room temp followed by the subsequent addition of agonist ligand in assay buffer. After agonist addition, cells were returned to a 37°/ 5% CO_2 incubator and functional responses were generated as indicated by the detection methods in the sections above. Competing concentration response curves for both competitor and agonist ligands were generated for each of the cAMP inhibition and β-arrestin2 recruitment assay protocols. Data were analyzed using global fitting to the Gaddum/Schild equation using a one site competition nonlinear regression analysis supplemented with linear regression plots of corresponding dose ratios using GraphPad Prism (GraphPad Software, San Diego, CA) (Arunlakshana and Schild, 1959; Kenakin, 2009).

In vivo

All studies were performed with 8 to 10-week-old male, C57BL/6 mice (Charles River Laboratories, Wilmington, MA) at Trevena, Inc. (King of Prussia, PA). β-arrestin1 ($\beta arr1^{-/-}$) and β-arrestin2 ($\beta arr2^{-/-}$) KO mice on the C57BL/6 background have been previously described (Bohn et al., 1999). In studies utilizing $\beta arr1^{-/-}$ and $\beta arr2^{-/-}$ mice, sex and weight matched control C57BL/6 mice (Sage Laboratories, Inc. Boyertown, PA) were utilized. Before beginning any experiments, mice were acclimated to the vivarium for at least 72 hours. During this time, mice were housed in standard conditions with 12-hour light/dark cycle, and fed ad libidum. Assays were approved by the Institutional Animal Care and Use Committee and were carried out in accordance with the Guide for the Care and Use of Laboratory Animals as adopted by the U.S. National Institutes of Health.

In vivo mechanical allodynia

The threshold for responses to punctate mechanical stimuli (mechanical allodynia) was tested according to the frequency method with slight modifications (Bonin et al., 2014). In brief, the plantar surface of the animal hind paw was stimulated with a single von Frey monofilament (0.4 g) for approximately 1-2 seconds. If there was a withdrawal response, it was recorded as a positive response. A response was defined as a lifting or shaking of the paw upon stimulation. This was repeated ten times for each mouse. The final measurement for each mouse is the % non-response to stimulation for the ten trials.

In vivo OIMA

Opioid-induced mechanical allodynia studies were designed and conducted based on previous reports (Chen et al., 2010; Hua et al., 2016). Briefly, mice were given subcutaneous (s.c.) injections of vehicle or μ-opioid agonists twice per day for four days. To induce allodynia, twice the dose corresponding to maximal efficacy in a hot plate antinociceptive assay was administered on days 1-3 while four times the maximal efficacious hot plate dose was given on day 4. On each of the four drug treatment days, prior to compound administration, a measurement of mechanical allodynia was obtained using the method described above. On the fifth day animals were again tested but with no additional drug treatments. This repeat dosing paradigm resulted in a dose-dependent increase in OIMA using oxycodone, a conventional MOPR agonist **(Supplemental Figure 1)**. For OIMA reversal studies, animals were switched on day 6 to a different μ-opioid agonist and again tested for mechanical allodynia for the next five days as described above. For experiments requiring osmotic pumps (Raehal and Bohn, 2011), pumps (Alzet model 2001, Durect Corporation, Cupertino, CA) were subcutaneously implanted through a small skin incision between the shoulder blades during a surgical procedure. Before implantation, compound or vehicle was loaded into the osmotic pumps according to the manufacturer's instructions. Briefly, under light isoflurane anesthesia a small incision was made with scissors and a small pocket was formed beneath the skin. The pump was then inserted and

the incision was closed using wound clips. To insure immediate drug delivery, osmotic pumps were submerged in 0.9% NaCl solution and incubated overnight at 37°C prior to implantation. The continuous infusion regimen aimed to administer a comparable amount of drug per day as the s.c. dosing regimen (average of 4 day dosing) and promote comparable analgesia (across MOPR ligands) in a hot plate assay.

To address the contribution of NOPR engagement in the development of OIH, cebranopadol (0.01 or 0.03 mg/kg s.c.; twice daily), a MOPR/NOPR-mixed agonist that lacks G protein-biased MOPR pharmacology, was also assessed in the OIMA model over 4 days of chronic dosing. This dose-range was selected to reflect doses previously used to characterize cebranopadol pharmacology (Schunk et al., 2014). Mechanical allodynia was measured as described above.

In vivo hot plate

The hot plate test is adapted from that described previously (Tyers, 1980). Animals were placed individually on a heated surface (56°C) and the time interval (seconds) between placement and a shaking, licking or tucking of the hind paw was recorded as the pre-drug latency. This same procedure was repeated 30 minutes after s.c. administration of compound in 10% ethanol, 10% Kolliphor EL, 80% sterile water for injection (10:10:80) or saline as appropriate. All compounds were administered s.c. in a volume of 1 ml/100 g, with volume adjustments made for mouse dosing. The cutoff time, designed to prevent injury to the animals, was 30 seconds (with vehicle latencies of approximately 5-15 seconds). The percent maximum possible antinociceptive effect [% maximum possible effect (MPE)] was determined using the formula:

Percent MPE: ((Post drug latency – baseline latency) / (30 – baseline latency)) x 100

The pre-drug latency of each animal and cutoff times noted above was used and the experimenter was blinded to the treatment of animals during behavioral observations.

In vivo pharmacokinetics

Pharmacokinetics studies were performed at ChemPartner Co. (Shanghai, China) under protocols reviewed and approved by their Institutional Care and Use Committee. Pharmacokinetic profiles of TRV0109101 were determined in mice, rats, dogs and cynomolgus monkeys by several routes of administration (**Supplemental Methods and Supplemental Table 3**). Plasma (all species) and brain levels (mouse) of TRV0109101 were determined using LC-MS/MS bioanalytical methods. Pharmacokinetic parameters were calculated using WinNonlin v6.2 software (Pharsight Corporation, CA); data are presented in Supplemental Table 3.

Statistical analyses

All statistical analyses were calculated using GraphPad Prism software. Unless otherwise indicated, all values are reported as mean ± SEM, and statistical significance was determined using One-Way ANOVA with Dunnett's post-hoc analyses to vehicle or Two-Way ANOVA with Bonferroni post-hoc analyses to vehicle. For behavioral studies, a minimal sample size of 8 in each group will have greater than 99% power to detect a difference in means, assuming a standard deviation of 20, using a two-group t-test with a 0.05 two-sided significance level.

JPET Fast Forward. Published on May 22, 2017 as DOI: 10.1124/jpet.117.241117
This article has not been copyedited and formatted. The final version may differ from this version.

RESULTS

β-arrestins and Opioid-induced Mechanical Allodynia

To test the contributions of β-arrestin1 and β-arrestin2 to the development of opioid-induced mechanical allodynia (OIMA) as a model of OIH, chronic minipump infusion of vehicle (saline, n = 8) or oxycodone (25 mg/kg/day, n = 8) was tested in WT, βarr1$^{-/-}$ and βarr2$^{-/-}$ mice **(Figure 1)**. The use of implanted osmotic minipumps promoted consistent drug exposure and mitigated the potential pro-nociceptive effects of opioid withdrawal, a common pitfall in studying and diagnosing OIH. Mechanical allodynia was measured using 0.4 gram von Frey filaments during 7 days of chronic minipump infusion **(Figure 1A-C)**. In WT mice, significant mechanical hypersensitivity developed following two days of oxycodone infusion and lasted throughout the dosing paradigm **(Figure 1A)**, an effect that was not seen in βarr1$^{-/-}$ **(Figure 1B)** or βarr2$^{-/-}$ animals **(Figure 1C)**. In conjunction, animals were tested 5 min following testing of mechanical allodynia in the hot-plate model (56°C) and response latencies recorded **(Figure 1D-F)**. In all strains tested, mice developed antinociceptive tolerance to oxycodone throughout the dosing paradigm. Similar results were obtained in a different cohort of βarr1$^{-/-}$ and βarr2$^{-/-}$ animals to morphine (48 mg/kg/day; n = 15), oxycodone (25 mg/kg/day; n = 8) and fentanyl (3.2 mg/kg/day; n = 8) in both mechanical allodynia and hot plate nociceptive responses **(Supplemental Figure 2 A-D)**.

TRV0109101 *In Vitro* Pharmacology

As β-arrestins appear to play a prominent role in opioid-induced mechanical allodynia, decreasing agonist-promoted β-arrestin recruitment may be an avenue for generating differentiated MOPR analgesics with reduced liability for the development of OIH. Previously, we are able to pharmacologically decouple MOPR-mediated analgesia from conventional opioid-induced adverse events such as respiratory depression and constipation using the G

JPET Fast Forward. Published on May 22, 2017 as DOI: 10.1124/jpet.117.241117
This article has not been copyedited and formatted. The final version may differ from this version.

protein-biased MOPR ligand oliceridine (TRV130) in rodents (DeWire et al., 2013). The aligned effect of genetic and pharmacologic interdiction of MOPR/β-arrestin pharmacology suggests that a G protein-biased MOPR ligand may be able to deliver robust analgesia while reducing the risk of the development of OIH.

Through previously reported lead optimization studies, we identified several structurally-related G protein-biased MOPR agonists including {2-[(9R)-9-(Pyridin-2-yl)-6-oxaspiro[4.5]decan-9-yl]ethyl}-(thiophen-2-ylmethyl)amine (R-19; TRV0109101) **(Figure 2A)** (Chen et al., 2013; DeWire et al., 2013). Like oliceridine, TRV0109101 does not share any structural similarity to conventional opioid receptor modulators and is chemically distinct from recently identified G protein-biased MOPR ligands, PZM21 and mitragynine pseudoindoxyl. TRV0109101 promotes potent (10 nM) and robust $G\alpha_i$ activation (approximately 81% compared to morphine) while exhibiting significantly reduced agonist-promoted β-arrestin2 recruitment (23%) **(Figure 2B, Supplemental Table 1)**. Since GRK-mediated receptor phosphorylation contributes to β-arrestin/receptor interaction and β-arrestin function (receptor endocytosis), we monitored agonist-promoted hMOPR phosphorylation and receptor internalization. As expected of a G protein-biased MOPR ligand, TRV0109101 exhibited markedly lower G protein receptor kinase (GRK)-mediated hMOPR phosphorylation at serine 375 and hMOPR internalization as compared to conventional opioids **(Figures 3A, B)**. Further, we studied the nature of TRV0109101 interaction with the receptor in reference to other MOPR ligands by functional competition analysis. Thus, if TRV0109101 is functionally competitive with the MOPR antagonist naloxone, the EC_{50} of TRV0109101 will increase as the antagonist concentration is titrated higher while the maximal response to TRV0109101 remains the same. Indeed, increasing concentrations of naloxone exhibited a functionally competitive relationship with TRV0109101-promoted $G\alpha_i$ activity **(Figure 3C)**. Concordantly, increasing concentrations of TRV0109101 was functionally competitive with DAMGO-promoted β-arrestin2 recruitment **(Figure 3D)**. Schild

JPET Fast Forward. Published on May 22, 2017 as DOI: 10.1124/jpet.117.241117
This article has not been copyedited and formatted. The final version may differ from this version.

analysis of these data suggests that TRV0109101 operates through the common orthosteric ligand binding site used by conventional MOPR ligands with an approximate apparent K_D of 70 nM **(Figures 3C, D)**. TRV0109101 is MOPR selective (over NOPR, DOPR and KOPR) **(Figure 2C, Supplemental Tables 1 and 2)** and can activate MOPR across species **(Supplemental Table 1)**.

TRV0109101 *In Vivo* Pharmacology

Similar to oliceridine (TRV130), TRV0109101 promoted robust analgesia in multiple models of acute pain, such as hot plate (mouse [ED_{50} = 1.1 mg/kg] and rat [ED_{50} = 0.3 mg/kg]), tail flick (rat [ED_{50} = 0.09 mg/kg]) and incisional pain (rat) **(Figure 4A; Supplemental Figures 3, 4)** (DeWire et al., 2013). TRV0109101 administration exhibited a broad therapeutic window between analgesia and inhibition of gastrointestinal function, as measured by colonic propulsion (mouse [ED_{50} = 9.4 mg/kg, 8.5x greater than hotplate ED_{50}]) and fecal boli accumulation (mouse [ED_{50} = 6.3 mg/kg, 5.7x greater than hotplate ED_{50}]) assays **(Figure 4B-D).** The magnitude of this therapeutic window was greater than that reported for morphine and comparable to the window previously observed for oliceridine (DeWire et al., 2013).

TRV0109101 Pharmacokinetics

To understand the relationship between drug exposure and antinociceptive efficacy, pharmacokinetic profiling of TRV0109101 was conducted following a single i.v., s.c. and p.o. administration in male C57BL/6 mice. In addition to mouse, the pharmacokinetic profile of TRV0109101 was determined in rats, dogs and cynomolgus monkeys by various routes of administration (**Supplemental Methods and Supplemental Table 3**). In mice, TRV0109101 was rapidly absorbed following a s.c. dose, with a mean C_{max} of 1,560 ng/mL measured 30 min post-dose, peak brain exposure also observed 30 minutes post-dose and a $t_{1/2}$ of 0.8 hours (**Supplemental Table 3 and Supplemental Figure 5**). Data from mouse PK studies were used

to inform dosing regimens, drug administration routes and experimental protocols. For example, considering the T_{max}, all thermal antinociceptive assays after s.c. administration were performed at 30 min post-dose. Additionally, since the $t_{1/2}$ of TRV0109101 is estimated at 0.8 hours (s.c.), opioid-induced mechanical allodynia was measured approximately 12 hours after s.c. dosing to reduce any antiallodynic contribution of MOPR activation.

In summary, the pharmacokinetic profile of TRV0109101 supports the antinociceptive pharmacodynamics observed in rodents. Unbound brain concentrations of TRV0109101 were not determined; however, the estimated free plasma concentrations at minimum efficacious doses in the rodent models exceed the potency at the mouse and rat MOPR receptor.

TRV0109101 and Opioid-Induced Mechanical Allodynia

To test whether a G protein biased MOPR agonist induces OIMA, mice were chronically infused (minipump) with either vehicle (saline, n = 30), morphine (48 mg/kg/day, n = 8), oxycodone (25 mg/kg/day, n = 12), fentanyl (3.2 mg/kg/day, n = 8) or TRV0109101 (20 mg/kg/day; n = 8) over 7 days. Mechanical allodynia was measured using 0.4 gram von Frey filaments during 7 days of chronic minipump infusion. Significant mechanical allodynia developed following two days of oxycodone, morphine and fentanyl infusion, but not after TRV0109101 **(Figure 5A)**. This allodynia lasted throughout the dosing paradigm. In conjunction, 5 min after testing mechanical allodynia animals were tested in the hot-plate model (56°C) and response latencies recorded **(Figure 5B)**. In this assay, mice developed antinociceptive tolerance to oxycodone, morphine, fentanyl and TRV0109101, at the doses tested, throughout the experimental paradigm.

In addition, we adopted a twice daily s.c. dosing protocol on days 1-3, followed by a double dose on day 4 based on previous work (Chen et al., 2010). Mice were dosed with either vehicle (saline or 10:10:80; n = 16), morphine (day 1-3: 20 mg/kg; day 4: 40 mg/kg; n = 16),

JPET Fast Forward. Published on May 22, 2017 as DOI: 10.1124/jpet.117.241117
This article has not been copyedited and formatted. The final version may differ from this version.

oxycodone (day 1-3: 12 mg/kg; day 4: 24 mg/kg; n = 16), fentanyl (day 1-3: 0.6 mg/kg; day 4: 1.2 mg/kg; n = 16), or TRV0109101 (day 1-3: 20 mg/kg; day 4: 40 mg/kg; n = 8) **(Supplemental Figure 6)**. In this experiment, mechanical allodynia was measured using 0.4 gram von Frey filaments during 5 days of treatment and mice treated with oxycodone, morphine or fentanyl developed OIMA while TRV0109101 treated animals did not. Taken together these data suggest that chronic opioid dosing (morphine, oxycodone and fentanyl) leads to the induction of OIMA while dosing TRV0109101, a G protein-biased MOPR agonist, does not. Tolerance however, regardless of drug class, continued to develop suggesting that OIH and antinociceptive tolerance are governed by divergent mechanisms.

TRV0109101 Reversal of Opioid-Induced Mechanical Allodynia

We next tested whether morphine-induced mechanical allodynia could be reversed by switching drug treatments. We first established OIMA by treating mice, twice daily (s.c.), with either vehicle (saline; n = 12) or morphine (20 mg/kg; n = 12) for 4 days **(Figure 6 – Treatment A)**. Mechanical allodynia was measured daily and morphine treated animals began to display significant OIMA by day 2 and lasted throughout this 4 day treatment period as compared to vehicle. On the fifth day, after testing for OIMA, mice in the morphine treatment group were then reassigned to one of three, twice daily dosing (*s.c.*), treatment groups; vehicle (saline; n = 12), morphine (20 mg/kg; n = 12) or TRV0109101 (20 mg/kg, n = 12) for 7 additional days **(Figure 6 – Treatment B)**. Following the transition to Treatment B, morphine/vehicle and morphine/morphine-treated animals maintained OIMA levels throughout the entire testing period. In contrast, the morphine/TRV0109101-treated group initially developed OIMA whilst under the morphine regimen; however, this OIMA was attenuated when the treatment switched to TRV0109101. This OIMA reversal was not significantly different from vehicle/vehicle treated animals within 24 hours of initiating TRV0109101 treatment. Additional studies were performed in a new cohort of animals using fentanyl (0.2 mg/kg, 5 days of twice daily (s.c.) dosing) instead

JPET Fast Forward. Published on May 22, 2017 as DOI: 10.1124/jpet.117.241117
This article has not been copyedited and formatted. The final version may differ from this version.

of morphine to induce OIMA. In addition, we reduced TRV0109101 administration to pharmacologically-relevant doses, as determined by hot plate antinociception **(Supplemental Fig. 7)**. In these experiments, fentanyl-induced allodynia was fully reversed 1 day following **(Supplemental Figure 7 – Treatment A)** 1 mg/kg (n = 8) or 3 mg/kg TRV0109101 administration (twice daily, s.c.; n = 8). OIMA reversal was maintained throughout the dosing paradigm. **(Supplemental Figure 7A – Treatment B)** that was indistinguishable from vehicle/vehicle (n = 8) treated animals on days 7 and 8. Interestingly, animals initially on 3 mg/kg TRV0109101 (n = 8) did not develop OIMA (similar to 20 mg/kg in **Figure 6)**, but when switched to twice daily (s.c.) fentanyl treatment, developed OIMA by day 8 comparable to OIMA observed with fentanyl alone **(**0.6 mg/kg, **Supplemental Fig. 7)**. Five minutes after assessing mechanical allodynia, animals were tested in the hot-plate model (56°C) and response latencies recorded **(Supplemental Figure 7B)**. In this assay, mice developed antinociceptive tolerance to both fentanyl and TRV0109101, at the doses tested, throughout the experimental paradigm. Although switching to TRV0109101 rescues OIMA, cross-tolerance to different MOPR agonists is observed. Taken together these data confirm that in mice both morphine- and fentanyl-induced allodynia can be abrogated by switching to a TRV0109101 treatment paradigm but antinociceptive-tolerance may be regulated by a distinct mechanism.

JPET Fast Forward. Published on May 22, 2017 as DOI: 10.1124/jpet.117.241117
This article has not been copyedited and formatted. The final version may differ from this version.

DISCUSSION

Previous work using β-arrestin2 KO mice has established a role for β-arrestins in opioid-associated adverse events such as respiratory depression and reduced gastrointestinal function (Bohn et al., 1999; Raehal et al., 2005). These data supported the rationale for the discovery and development of G protein-biased MOPR agonists, such as oliceridine, as differentiated analgesics that promote antinociception with reduced liability for conventional opioid-induced adverse events. Here we show that chronic administration of oxycodone, morphine or fentanyl induce OIMA, a model of OIH, in WT, but not βarr1$^{-/-}$ and βarr2$^{-/-}$ mice while drug tolerance still developed in all genotypes. These data suggest that, in addition to its contributions to a number of characterized opioid-associated adverse events, β-arrestins are critical regulators of the development of OIMA independent of antinociceptive tolerance. We hypothesized that a G protein-biased MOPR agonist could differentiate from conventional opioids when monitoring the development of mechanical allodynia. Indeed, TRV0109101, a G protein-biased MOPR-selective agonist and analogue of oliceridine, did not promote the development of mechanical allodynia. In addition, TRV0109101 administration after induction of OIMA (using morphine or fentanyl) resulted in full rescue from established allodynia. Although previous work presented conflicting roles for β-arrestins in the development of OIH (Rowan et al., 2014a; Rowan et al., 2014b; Chen et al., 2016), our observations in a model of opioid-induced hyperalgesia, OIMA, provide strong support for the hypothesis that OIH is mediated, at least in part, via β-arrestin-dependent pathways and a G protein-biased MOPR agonist may be an advantageous approach to delivering robust analgesia while reducing the development of OIH.

TRV01019101 is a G protein-biased agonist among a new class of MOPR ligands that include oliceridine, PZM21 and mitragynine pseudoindoxyl. Reported G protein-biased MOPR agonists do not share structural similarity with conventional opioids and promote more effective coupling to G protein signaling pathways (associated with analgesia) than to β-arrestin

recruitment (associated with opioid-induced adverse events) as compared to morphine. In preclinical models of acute pain and opioid-associated adverse events, G protein-biased MOPR ligands exhibit an increased therapeutic window (compared to morphine) between analgesia and opioid-induced respiratory depression and reduced gastrointestinal function (DeWire et al., 2013; Manglik et al., 2016; Varadi et al., 2016). Although opioid-induced respiratory depression and constipation were improved for each biased ligand compared to morphine, observed effects on tolerance and abuse liability have not been consistent among this new class of MOPR modulators. These observations may be attributed to additional pharmacological target engagement independent of MOPR activity (DeWire et al., 2013; Manglik et al., 2016; Varadi et al., 2016). To date, only oliceridine has been evaluated in humans; multiple randomized controlled trials have suggested that oliceridine may have a wider therapeutic window than morphine (Soergel et al., 2014; Siuda et al., 2016). Like oliceridine, TRV0109101 is a G protein-biased, MOPR-selective agonist that demonstrates differentiation from morphine on measures of gastrointestinal function while promoting analgesia across multiple models of acute pain. Due to a pharmacodynamic and pharmacokinetic profile similar to oliceridine, we believe that TRV0109101 can serve as a representative pharmacophore for comparable compounds currently in clinical development to further assess the differentiation of a G protein-biased MOPR agonist compared to conventional opioids.

Since morphine, fentanyl and oxycodone were unable to promote OIMA in $\beta arr1^{-/-}$ and $\beta arr2^{-/-}$ mice, β-arrestins may play a fundamental role in the development of OIH and corroborate that the use of a G protein-biased MOPR agonist could avoid the development of OIH. In stark contrast to conventional opioids, TRV0109101 did not induce significant OIMA at any point during the observed time course, even when administered at supratherapeutic doses. TRV0109101 also demonstrated the ability to rapidly rescue morphine and fentanyl-induced mechanical allodynia. TRV0109101-promoted reversal of OIMA was observed after the first

administered dose and accomplished sustained, full reversal throughout the dosing paradigm. Interestingly, chronic administration of TRV0109101 and subsequent switching to fentanyl resulted in the induction of mechanical allodynia. These data suggest that agonist-promoted β-arrestin recruitment appears to play a prominent role in not only the development of OIH, but also the maintenance of the condition. Thus, as a G protein-biased agonist, TRV0109101 fundamentally avoids the contributions of β-arrestins in these processes at the receptor level to promote robust MOPR-mediated analgesia with reduced OIH liability.

Although our pharmacological (TRV0109101) and genetic ($\beta arr1^{-/-}$ and $\beta arr2^{-/-}$ mice) approaches suggest that β-arrestin engagement mediates the development of OIH, we have yet to study the direct contributions of NOPR engagement to the differentiated pharmacology of TRV0109101. Interestingly, cebranopadol (Schunk et al., 2014), a MOPR/NOPR-mixed agonist that lacks G protein-biased MOPR pharmacology, induced robust mechanical allodynia (comparable to oxycodone) after chronic dosing **(Supplemental Figure 8)**. These data, along with the congruent pharmacological and genetic evidence presented, suggest that β-arrestin recruitment to MOPR is a primary determinant in the development of opioid-induced hyperalgesia

While not inducing OIMA at the doses tested, TRV0109101 promoted drug tolerance comparable to conventional opioids. Interestingly, mitragynine pseudoindoxyl, a recently developed MOPR agonist/DOPR antagonist with limited activity at β-arrestin2, also displayed analgesic tolerance in the tail flick assay. In contrast to other MOPR ligands, mitragynine pseudoindoxyl-induced tolerance developed substantially slower (29 days v. 5 days) than morphine when dosed twice daily (5 mg/kg, twice daily, s.c.) (Varadi et al., 2016). As mitragynine pseudoindoxyl also serves as a DOPR antagonist, it is possible that this activity may contribute to observations of delayed tolerance. It will be important to examine

TRV0109101 at different doses and in other models of acute pain to better examine drug tolerance among G protein-biased MOPR agonists.

A striking observation described in this work regards the critical role that β-arrestins play in the development of OIMA independent of modulating drug tolerance. This suggests that the development of OIH and opioid tolerance may operate through fundamentally distinct mechanisms. Although previous work has suggested that morphine does not promote antinociceptive tolerance in βarr2$^{-/-}$ mice following once daily morphine (10 mg/kg/day, *s.c.*) injections (Bohn et al., 2000; Bohn et al., 2002), our dosing paradigm reveals that morphine, oxycodone and fentanyl promote tolerance independent of β-arrestin expression. While comparable tolerance to oxycodone and fentanyl infusion was observed in βarr2$^{-/-}$ mice (Raehal and Bohn, 2011), delayed morphine tolerance was noted in βarr2$^{-/-}$ mice using a tail flick antinociceptive assay, a measure of spinal reflexive responsiveness (Bohn et al., 2002). While βarr2 is believed to be involved in MOPR desensitization, it has been extensively examined in opioid tolerance, dependence and OIH (Chen et al., 2016). βarr1 is thought to play a role in MOPR ubiquitination, dephosphorylation and resensitization (Dang et al., 2011; Groer et al., 2011; Dang and Christie, 2012; Williams et al., 2013; Raehal and Bohn, 2014) but little is known about its role in opioid-induced adverse events. As such, it is currently unclear whether the actions of βarr1 and βarr2 in OIH are mediated by distinct cellular mechanisms, or if possible compensatory mechanisms present in knockout animals overshadow their singular contributions. Previous studies have also attributed β-arrestins with MOPR-mediated adverse events in both humans and animals, with particular emphasis on respiratory depression, gastrointestinal transit, reward reinforcement, tolerance and now OIH (Bohn et al., 1999; Bohn et al., 2000; Raehal et al., 2005; DeWire et al., 2013; Soergel et al., 2014; Manglik et al., 2016; Varadi et al., 2016).

The clinical approach for treating opioid tolerance is markedly different than addressing OIH. Tolerance may be overcome by increasing the drug dose or by “opioid-switching” (Lee et al., 2011). “Opioid-switching” is a common clinical practice where different opioids used to manage pain are sometimes changed to maintain analgesic efficacy without subsequent opioid-induced adverse consequences including tolerance (Quigley, 2004; Mercadante and Bruera, 2006; Mercadante and Bruera, 2016). Although these protocols may improve antinociceptive tolerance, they are unlikely to improve the pain associated with OIH. Pain associated with OIH escalates with increased opioid dosage and conventional opioids, such as morphine, fentanyl and oxycodone, appear to carry a comparable liability for the development of OIH (Lee et al., 2011). As chronic dosing of TRV0109101 did not result in OIMA and switching to TRV0109101 could reverse fentanyl or morphine-promoted OIMA, an “opioid-switching” protocol to a G protein-biased MOPR agonist, rather than a conventional opioid, could be an advantageous avenue in treating pain in patients with established OIH. Although we believe that the reversal of fentanyl or morphine- promoted OIMA using TRV0109101 is consistent with the differentiated biased ligand mechanism of action, we have not ruled out that opioid-switching alone may explain this observation. Future studies monitoring a variety of opioids and dosing regimens could be useful to better characterize this phenomenon.

In conclusion, we believe that other G protein-biased MOPR agonists, under these treatment conditions, may demonstrate analogous properties to TRV0109101 including decreased liability for the development of OIH in mice as compared to conventional opioids. Whether these findings translate into the clinic is yet to be determined, but it remains an interesting area for future investigation. Broadly, this preponderance of data, along with the preclinical and clinical characterization of oliceridine, validate that the development of biased agonists to selectively target one intracellular signaling pathway over another is an important approach toward providing clinical efficacy with reduced adverse event liability.

ACKNOWLEDGEMENTS

The authors would like to thank Michael Kramer (Trevena, Inc.) for assisting the interpretation of pharmacokinetic data and Dr. David Clark (Stanford University) for critical reading of the manuscript.

AUTHOR CONTRIBUTIONS

Participated in research design: Koblish, Carr III, Siuda, Rominger, Gowen-MacDonald, Cowan, Crombie, Violin, Lark

Conducted experiments: Koblish, Carr III, Siuda, Rominger, Gowen-MacDonald

Contributed new reagents or analytic tools: Gowen-MacDonald

Performed data analysis: Koblish, Carr III, Siuda, Rominger, Gowen-MacDonald, Cowan

Wrote or contributed to the writing of the manuscript: Koblish, Carr III, Siuda, Rominger, Gowen-MacDonald, Crombie, Violin, Lark

REFERENCES

Angst MS and Clark JD (2006) Opioid-induced hyperalgesia: a qualitative systematic review. *Anesthesiology* **104**:570-587.

Arunlakshana O and Schild HO (1959) Some quantitative uses of drug antagonists. *British journal of pharmacology and chemotherapy* **14**:48-58.

Bohn LM, Gainetdinov RR, Lin FT, Lefkowitz RJ and Caron MG (2000) Mu-opioid receptor desensitization by beta-arrestin-2 determines morphine tolerance but not dependence. *Nature* **408**:720-723.

Bohn LM, Lefkowitz RJ and Caron MG (2002) Differential mechanisms of morphine antinociceptive tolerance revealed in (beta)arrestin-2 knock-out mice. *J Neurosci* **22**:10494-10500.

Bohn LM, Lefkowitz RJ, Gainetdinov RR, Peppel K, Caron MG and Lin FT (1999) Enhanced morphine analgesia in mice lacking beta-arrestin 2. *Science* **286**:2495-2498.

Bonin RP, Bories C and De Koninck Y (2014) A simplified up-down method (SUDO) for measuring mechanical nociception in rodents using von Frey filaments. *Mol Pain* **10**:26.

Chen G, Xie RG, Gao YJ, Xu ZZ, Zhao LX, Bang S, Berta T, Park CK, Lay M, Chen W and Ji RR (2016) beta-arrestin-2 regulates NMDA receptor function in spinal lamina II neurons and duration of persistent pain. *Nat Commun* **7**:12531.

Chen X-T, Pitis P, Liu G, Yuan C, Gotchev D, Cowan CL, Rominger DH, Koblish M, DeWire SM, Crombie AL, Violin JD and Yamashita DS (2013) Structure–Activity Relationships and Discovery of a G Protein Biased μ Opioid Receptor Ligand, [(3-Methoxythiophen-2-yl)methyl]({2-[(9R)-9-(pyridin-2-yl)-6-oxaspiro-[4.5]decan-9-yl]ethyl})amine (TRV130), for the Treatment of Acute Severe Pain. *Journal of Medicinal Chemistry* **56**:8019-8031.

Chen Y, Yang C and Wang ZJ (2010) Ca2+/calmodulin-dependent protein kinase II alpha is required for the initiation and maintenance of opioid-induced hyperalgesia. *J Neurosci* **30**:38-46.

Chu LF, Angst MS and Clark D (2008) Opioid-induced hyperalgesia in humans: molecular mechanisms and clinical considerations. *The Clinical journal of pain* **24**:479-496.

Chu LF, Clark DJ and Angst MS (2006) Opioid Tolerance and Hyperalgesia in Chronic Pain Patients After One Month of Oral Morphine Therapy: A Preliminary Prospective Study. *The Journal of Pain* **7**:43-48.

Compton P, Canamar CP, Hillhouse M and Ling W (2012) Hyperalgesia in Heroin Dependent Patients and the Effects of Opioid Substitution Therapy. *The Journal of Pain* **13**:401-409.

Compton P, Charuvastra VC and Ling W (2001) Pain intolerance in opioid-maintained former opiate addicts: effect of long-acting maintenance agent. *Drug Alcohol Depend* **63**:139-146.

Corder G, Tawfik VL, Wang D, Sypek EI, Low SA, Dickinson JR, Sotoudeh C, Clark JD, Barres BA, Bohlen CJ and Scherrer G (2017) Loss of mu opioid receptor signaling in nociceptors, but not microglia, abrogates morphine tolerance without disrupting analgesia. *Nature medicine* **23**:164-173.

Dang VC, Chieng B, Azriel Y and Christie MJ (2011) Cellular morphine tolerance produced by betaarrestin-2-dependent impairment of mu-opioid receptor resensitization. *J Neurosci* **31**:7122-7130.

Dang VC and Christie MJ (2012) Mechanisms of rapid opioid receptor desensitization, resensitization and tolerance in brain neurons. *British Journal of Pharmacology* **165**:1704-1716.

DeWire SM, Yamashita DS, Rominger DH, Liu G, Cowan CL, Graczyk TM, Chen X-T, Pitis PM, Gotchev D, Yuan C, Koblish M, Lark MW and Violin JD (2013) A G Protein-Biased Ligand at the μ-Opioid Receptor Is Potently Analgesic with Reduced Gastrointestinal and

Respiratory Dysfunction Compared with Morphine. *Journal of Pharmacology and Experimental Therapeutics* **344**:708-717.

Eastman P, Le BH, Grant I and Berry S (2014) Is opioid-induced hyperalgesia a genuine issue for palliative care patients and clinicans? *Journal of Clinical Oncology* **32**:197-197.

Gomes T, Mamdani MM, Paterson JM, Dhalla IA and Juurlink DN (2014) Trends in high-dose opioid prescribing in Canada. *Canadian family physician Medecin de famille canadien* **60**:826-832.

Groer CE, Schmid CL, Jaeger AM and Bohn LM (2011) Agonist-directed interactions with specific beta-arrestins determine mu-opioid receptor trafficking, ubiquitination, and dephosphorylation. *J Biol Chem* **286**:31731-31741.

Guignard MDB, Bossard MDAnne E, Coste MDC, Sessler MDDaniel I, Lebrault MDC, Alfonsi MDP, Fletcher MDD and Chauvin MDM (2000) Acute Opioid ToleranceIntraoperative Remifentanil Increases Postoperative Pain and Morphine Requirement. *Anesthesiology* **93**:409-417.

Hua Z, Liu L, Shen J, Cheng K, Liu A, Yang J, Wang L, Qu T, Yang H, Li Y, Wu H, Narouze J, Yin Y and Cheng J (2016) Mesenchymal Stem Cells Reversed Morphine Tolerance and Opioid-induced Hyperalgesia. *Scientific reports* **6**:32096.

Johannes CB, Le TK, Zhou X, Johnston JA and Dworkin RH (2010) The prevalence of chronic pain in United States adults: results of an Internet-based survey. *J Pain* **11**:1230-1239.

Johnson JL, Rolan PE, Johnson ME, Bobrovskaya L, Williams DB, Johnson K, Tuke J and Hutchinson MR (2014) Codeine-induced hyperalgesia and allodynia: investigating the role of glial activation. *Translational psychiatry* **4**:e482.

Kenakin T (2009) *A pharmacology primer: theory, application and methods*. Academic Press.

Lee M, Silverman SM, Hansen H, Patel VB and Manchikanti L (2011) A comprehensive review of opioid-induced hyperalgesia. *Pain Physician* **14**:145-161.

Lipman JJ and Blumenkopf B (1989) Comparison of subjective and objective analgesic effects of intravenous and intrathecal morphine in chronic pain patients by heat beam dolorimetry. *Pain* **39**:249-256.

Manglik A, Lin H, Aryal DK, McCorvy JD, Dengler D, Corder G, Levit A, Kling RC, Bernat V, Hubner H, Huang XP, Sassano MF, Giguere PM, Lober S, Da D, Scherrer G, Kobilka BK, Gmeiner P, Roth BL and Shoichet BK (2016) Structure-based discovery of opioid analgesics with reduced side effects. *Nature*:1-6.

Marion Lee M, Sanford Silverman M, Hans Hansen M and Vikram Patel M (2011) A comprehensive review of opioid-induced hyperalgesia. *Pain physician* **14**:145-161.

Mauermann E, Filitz J, Dolder P, Rentsch KM, Bandschapp O and Ruppen W (2016) Does Fentanyl Lead to Opioid-induced Hyperalgesia in Healthy Volunteers?A Double-blind, Randomized, Crossover Trial. *Anesthesiology* **124**:453-463.

Mercadante S and Bruera E (2006) Opioid switching: a systematic and critical review. *Cancer treatment reviews* **32**:304-315.

Mercadante S and Bruera E (2016) Opioid switching in cancer pain: From the beginning to nowadays. *Critical reviews in oncology/hematology* **99**:241-248.

Quigley C (2004) Opioid switching to improve pain relief and drug tolerability. *Cochrane Database of Systematic Reviews*.

Raehal KM and Bohn LM (2011) The role of beta-arrestin2 in the severity of antinociceptive tolerance and physical dependence induced by different opioid pain therapeutics. *Neuropharmacology* **60**:58-65.

Raehal KM and Bohn LM (2014) beta-arrestins: regulatory role and therapeutic potential in opioid and cannabinoid receptor-mediated analgesia. *Handbook of experimental pharmacology* **219**:427-443.

Raehal KM, Walker JK and Bohn LM (2005) Morphine side effects in beta-arrestin 2 knockout mice. *J Pharmacol Exp Ther* **314**:1195-1201.

Rowan MP, Bierbower SM, Eskander MA, Szteyn K, Por ED, Gomez R, Veldhuis N, Bunnett NW and Jeske NA (2014a) Activation of mu opioid receptors sensitizes transient receptor potential vanilloid type 1 (TRPV1) via beta-arrestin-2-mediated cross-talk. *PLoS One* **9**:e93688.

Rowan MP, Szteyn K, Doyle AP, Gomez R, Henry MA and Jeske NA (2014b) beta-arrestin-2-biased agonism of delta opioid receptors sensitizes transient receptor potential vanilloid type 1 (TRPV1) in primary sensory neurons. *Mol Pain* **10**:50.

Seymour RA, Rawlins MD and Rowell FJ (1982) DIHYDROCODEINE-INDUCED HYPERALGESIA IN POSTOPERATIVE DENTAL PAIN. *The Lancet* **319**:1425-1426.

Simonnet G and Rivat C (2003) Opioid-induced hyperalgesia: abnormal or normal pain? *NeuroReport* **14**:1-7.

Siuda ER, Carr R, 3rd, Rominger DH and Violin JD (2016) Biased mu-opioid receptor ligands: a promising new generation of pain therapeutics. *Current opinion in pharmacology* **32**:77-84.

Schunk S, Linz K, Frormann S, Hinze C, Oberbörsch S, Sundermann B, Zemolka S, Englberger W,Germann T, Christoph T, Kögel Y, Schröder W, Harlfinger S, Saunders D, Kless Schick H, and Sonnenschein H (2014) Discovery of Spiro[cyclohexanedihydropyrano[3,4-b]indole]-amines as Potent NOP and Opioid Receptor Agonists. *ACS Med Chem Lett* **5**: 851–856

Soergel DG, Subach RA, Burnham N, Lark MW, James IE, Sadler BM, Skobieranda F, Violin JD and Webster LR (2014) Biased agonism of the mu-opioid receptor by TRV130 increases analgesia and reduces on-target adverse effects versus morphine: A randomized, double-blind, placebo-controlled, crossover study in healthy volunteers. *Pain* **155**:1829-1835.

Trang T, Al-Hasani R, Salvemini D, Salter MW, Gutstein H and Cahill CM (2015) Pain and Poppies: The Good, the Bad, and the Ugly of Opioid Analgesics. *The Journal of Neuroscience* **35**:13879-13888.

Tyers MB (1980) A classification of opiate receptors that mediate antinociception in animals. *Br J Pharmacol* **69**:503-512.

Varadi A, Marrone GF, Palmer TC, Narayan A, Szabo MR, Le Rouzic V, Grinnell SG, Subrath JJ, Warner E, Kalra S, Hunkele A, Pagirsky J, Eans SO, Medina JM, Xu J, Pan YX, Borics A, Pasternak GW, McLaughlin JP and Majumdar S (2016) Mitragynine/corynantheidine pseudoindoxyls as opioid analgesics with mu agonism and delta antagonism which do not recruit beta-arrestin-2. *J Med Chem*.

Williams JT, Ingram SL, Henderson G, Chavkin C, von Zastrow M, Schulz S, Koch T, Evans CJ and Christie MJ (2013) Regulation of μ-Opioid Receptors: Desensitization, Phosphorylation, Internalization, and Tolerance. *Pharmacological Reviews* **65**:223-254.

FOOTNOTES

This work was supported by Trevena, Inc., a company discovering and developing investigational products targeting GPCRs, including oliceridine. All authors are present or former employees of Trevena, Inc.

Reprint requests can be addressed to Michael W. Lark at Trevena, Inc., 1018 West 8th Ave., Suite A, King of Prussia, PA 19406 or mlark@trevena.com.

JPET Fast Forward. Published on May 22, 2017 as DOI: 10.1124/jpet.117.241117
This article has not been copyedited and formatted. The final version may differ from this version.

FIGURE LEGENDS

Figure 1: WT, but not βarr1-KO and βarr2-KO mice, exhibit opioid-induced mechanical allodynia while all develop antinociceptive tolerance. Mechanical allodynia was measured over 7 days in WT **(A)**, βarr1-KO **(B)** and βarr2-KO **(C)** mice in response to chronic minipump infusion (7 days) with vehicle (saline, n = 8) or oxycodone (25 mg/kg/day, n = 8). 5 min after testing for mechanical allodynia, thermal (56°C) hot plate antinociceptive responses in WT **(D)**, βarr1-KO **(E)** and βarr2-KO **(F)** mice were measured. Data are mean ± SEM (*** $p < 0.001$ via Two Way Repeated Measures ANOVA with Bonferroni post-tests to vehicle).

Figure 2: TRV0109101 is a potent and MOPR-selective G protein biased agonist. {2-[(9R)-9-(Pyridin-2-yl)-6-oxaspiro[4.5]decan-9-yl]ethyl}-(thiophen-2-ylmethyl)amine, TRV0109101, **(A)**, promoted inhibition of cAMP accumulation (**B**, orange) with a notable reduction in β-arrestin recruitment (**B**, teal). **(C)** TRV0109101 exhibits marked selectivity for MOPR (orange) over KOPR (yellow), DOPR (blue) and NOPR (green). Data are mean ± SEM for at least 3 independent experiments.

Figure 3: TRV0109101 promotes less receptor phosphorylation and internalization than conventional opioids and is functionally competitive with other MOPR ligands. (A) In HEK293 cells stably overexpressing hMOPR, TRV0109101 exhibited significantly reduced agonist-promoted receptor phosphorylation at Ser^{375} as compared to morphine. **(B)** TRV0109101 promoted reduced internalization as compared to morphine and other MOPR agonists. Data are mean ± SEM for at least 3 independent experiments (* $p < 0.05$, via One Way ANOVA with Bonferroni's Multiple Comparison Test post-tests). **(C)** Functional competition analysis demonstrates that a MOPR-antagonist, naloxone, can competitively inhibit TRV9101-promoted inhibition of cAMP production. **(D)** Conversely, TRV0109101 is able to effectively

interdict DAMGO-promoted β-arrestin2 recruitment with an apparent KD of 70 nM. Data are mean ± SEM for at least 3 independent experiments.

Figure 4: TRV0109101 exhibits a robust therapeutic window between analgesia and inhibition of gastrointestinal output. Mice were injected s.c. with vehicle (grey) or TRV0109101 (blue) at the indicated doses and analyzed by: (A) a 56°C hot plate assay (vehicle: n = 8; TRV0109101: n = 4-8); (B) a four hour fecal boli accumulation assay (n = 8) or (C) a glass bead colonic motility assay (n = 6-8). (D) These same data are then expressed as %MPE and fit with nonlinear regression for ED_{50} determination. Data are mean ± SEM (* $p < 0.05$, *** $p < 0.001$ via One Way ANOVA with Dunnett's post-test to vehicle group.

Figure 5: Continuous TRV0109101 administration does not produce opioid-induced mechanical allodynia but does promote antinociceptive tolerance to thermal stimuli. (A) Mechanical allodynia was measured over 7 days in mice in response to a chronic minipump infusion (7 days) with vehicle (saline, n = 30), morphine (48 mg/kg/day, n = 8), oxycodone (25 mg/kg/day, n = 12), TRV0109101 (20 mg/kg/day; n = 8) or fentanyl (3.2 mg/kg/day, n = 8). **(B)** 5 min after testing for mechanical allodynia, thermal (56°C) hot plate antinociceptive responses were measured. Data are mean ± SEM (** $p < 0.01$, *** $p < 0.001$ via Two Way Repeated Measures ANOVA with Bonferroni post-tests to vehicle).

Figure 6: Repeated TRV0109101 administration reverses morphine-induced mechanical allodynia. Mechanical allodynia was measured following repeated morphine administration. Treatment A - Mice were dosed twice daily (s.c.) with vehicle (n = 12) or morphine for 4 days (20 mg/kg). Treatment B - On day 5 morphine treated mice were reassigned and dose twice daily (s.c.) to vehicle (saline; n = 12), morphine (20 mg/kg; n = 12) or TRV0109101 (20 mg/kg, n = 12) for 8 additional days. Data are mean ± SEM (* $p < 0.05$, ** $p <$

JPET Fast Forward. Published on May 22, 2017 as DOI: 10.1124/jpet.117.241117
This article has not been copyedited and formatted. The final version may differ from this version.

0.01, *** $p < 0.001$, via Two Way Repeated Measures ANOVA followed by Bonferroni's post-tests to vehicle).

JPET Fast Forward. Published on May 22, 2017 as DOI: 10.1124/jpet.117.241117
This article has not been copyedited and formatted. The final version may differ from this version.

FIGURE 1

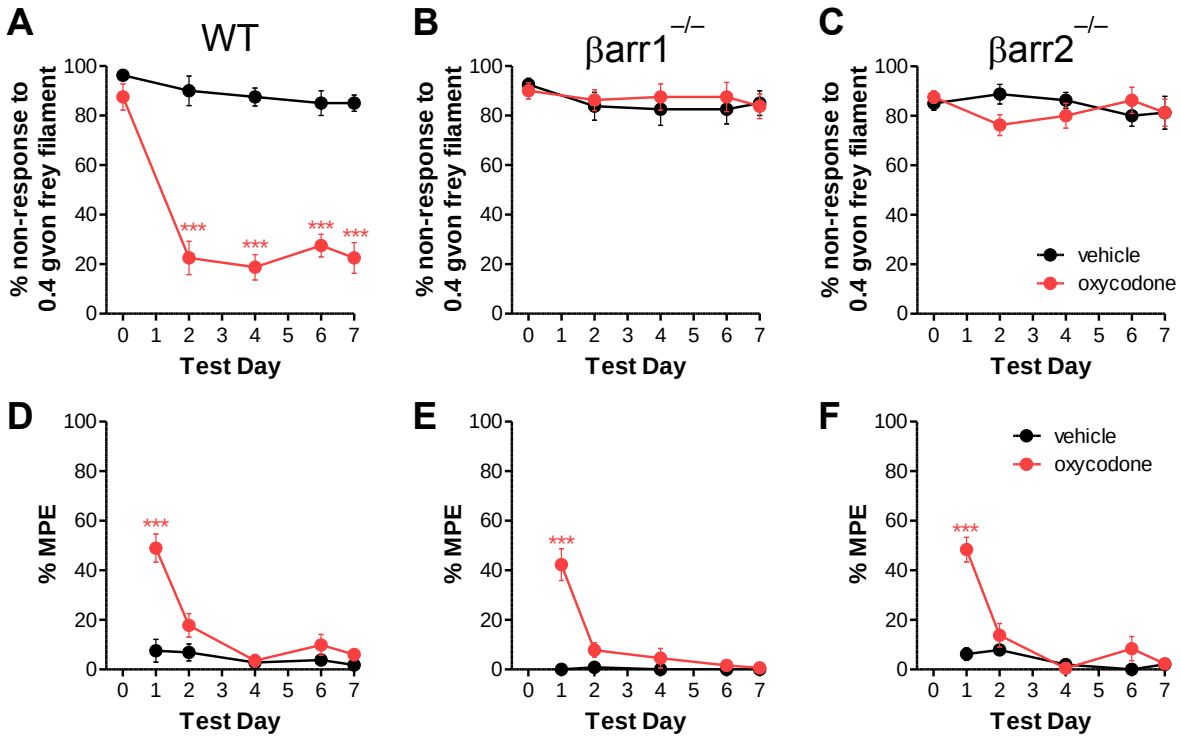

JPET Fast Forward. Published on May 22, 2017 as DOI: 10.1124/jpet.117.241117
This article has not been copyedited and formatted. The final version may differ from this version.

Figure 2

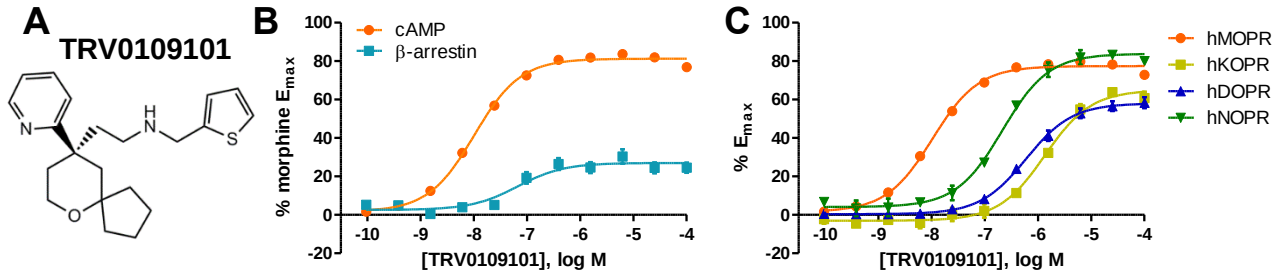

JPET Fast Forward. Published on May 22, 2017 as DOI: 10.1124/jpet.117.241117
This article has not been copyedited and formatted. The final version may differ from this version.

Figure 3

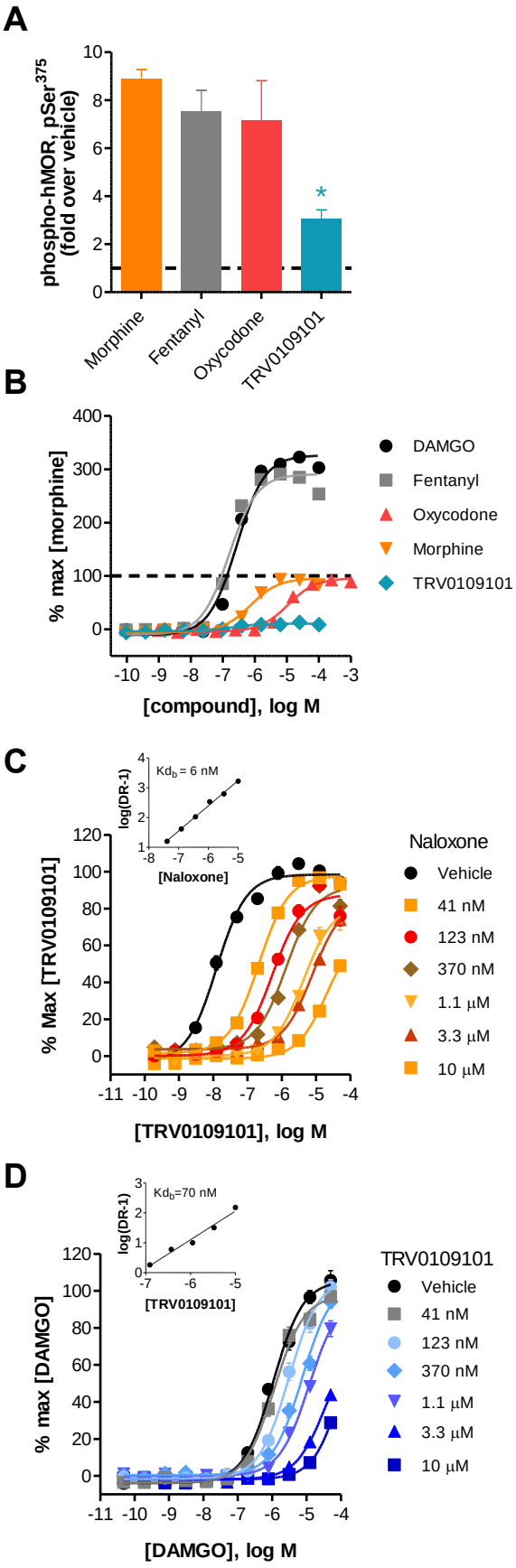

JPET Fast Forward. Published on May 22, 2017 as DOI: 10.1124/jpet.117.241117
This article has not been copyedited and formatted. The final version may differ from this version.

Figure 4

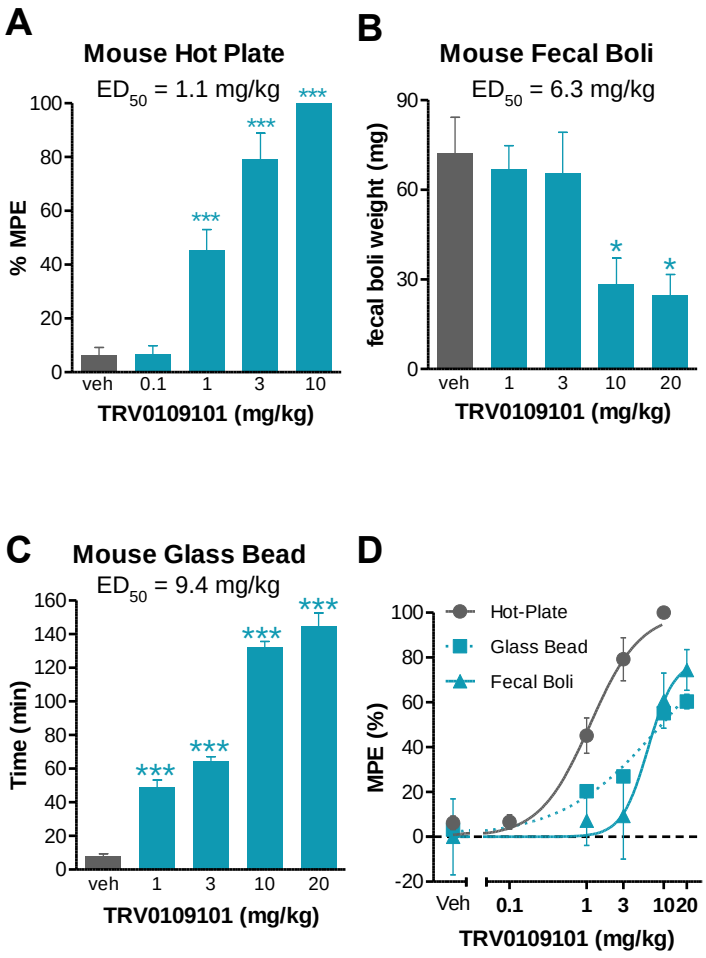

JPET Fast Forward. Published on May 22, 2017 as DOI: 10.1124/jpet.117.241117
This article has not been copyedited and formatted. The final version may differ from this version.

Figure 5

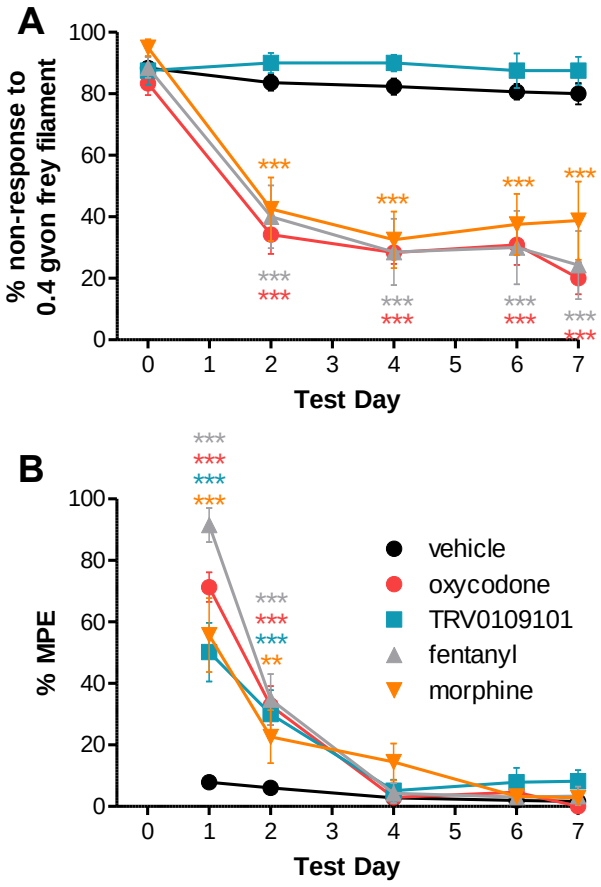

JPET Fast Forward. Published on May 22, 2017 as DOI: 10.1124/jpet.117.241117
This article has not been copyedited and formatted. The final version may differ from this version.

Figure 6

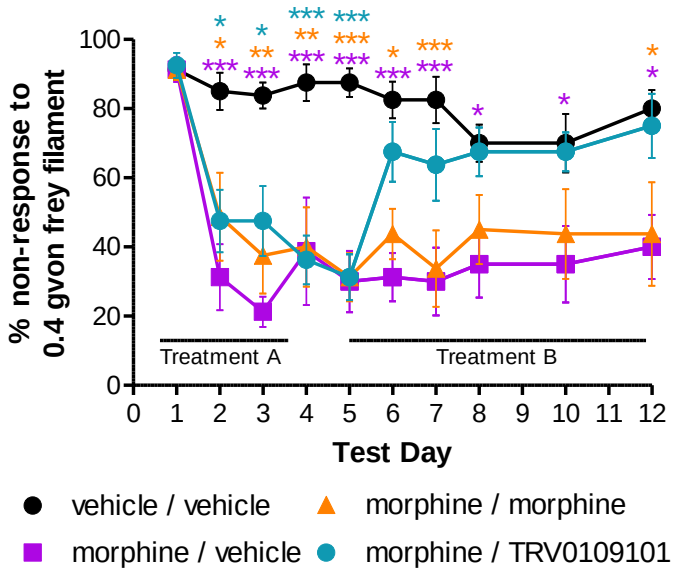

Supplemental Methods

Pharmacokinetics - Pharmacokinetic studies were performed at ChemPartner Co. (Shanghai, China), under protocols reviewed and approved by the Institutional Animal Care and Use Committee. The pharmacokinetic (PK) profile of TRV0109101 was evaluated in mice, rats, dogs, and cynomolgus monkeys by several routes of administration. Plasma (all species) and brain levels (mouse) of TRV0109101 were determined using LC-MS/MS bioanalytical methods. Pharmacokinetic parameters from all studies were calculated using WinNonlin v6.2 software (Pharsight Corporation, CA); data are presented in Supplemental Table 3.

Mouse PK studies - Studies were conducted to determine the PK and bioavailability of TRV0109101 following a single intravenous (i.v.), subcutaneous (s.c.) or oral gavage (p.o.) dose in male C57Bl/6 mice (n=24 per dose route). Dosing solutions were prepared by dissolving TRV0109101 in 10% ethanol and 10% cremophor and 80% sterile water. Mice received an i.v. dose of 3 mg/kg TRV0109101 in a 5 mL/kg dose volume, a s.c. dose of 10 mg/kg TRV0109101 in a 10 mL/kg dose volume, or a 10 mg/kg oral dose of TRV0109101 in a 10 mL/kg dose volume. Blood was collected into K2EDTA tubes predose and 0.083, 0.25, 0.5, 1, 2, 4 and 8 hr postdose via retro-orbital puncture from 3 mice per dose group and processed to plasma. Brain samples were collected and snap frozen on dry ice.

Rat PK studies -

Single administration studies

The pharmacokinetic profile of TRV0109101 was determined following a single i.v. or s.c. dose in male Sprague Dawley rats (n=3 per dose route). Dosing solutions were prepared by dissolving TRV0109101 in 10% ethanol and 10% cremophor and 80% sterile water. Rats received an i.v. dose of 3 mg/kg TRV0109101 in a 1 mL/kg dose volume, or a s.c. dose of 1 mg/kg TRV0109101 in a 1 mL/kg dose volume. Blood was collected into K2EDTA tubes predose and 0.083, 0.25, 0.5, 1, 2, 4 and 8 hr postdose via retro-orbital puncture from 3 rats per dose group and processed to plasma.

Intravenous infusion studies

The pharmacokinetic profile of TRV0109101 was determined following i.v. infusion in male Sprague Dawley rats (n=3). Dosing solutions were prepared by dissolving TRV0109101 in 5% ethanol, 5% cremophor and 90% D5W (5% dextrose in water). Rats were infused for 6 hours via the femoral vein with TRV0109101 at a rate of 2 or 5 mg/kg/hr. Blood was collected into K2EDTA tubes predose and 0.083, 0.25, 0.5, 1, 2, 4 and 8 hr postdose via implanted cannula in the jugular vein from 3 rats per dose group and processed to plasma.

Dog PK studies - The pharmacokinetic profile of TRV0109101 was determined following a single i.v. dose in male beagle dogs (n=3). Dosing solutions were prepared by dissolving TRV0109101 in 10% ethanol and 90% saline. Dogs received an i.v. dose of 1 mg/kg TRV0109101 via cephalic vein injection in a 1 mL/kg dose volume. Blood was collected into K2EDTA tubes predose and 0.083, 0.25, 0.5, 1, 2, 4, 8, 12 and 24 hr postdose from a cephalic or saphenous vein and processed to plasma.

Monkey PK studies - The pharmacokinetic profile of TRV0109101 was determined following a single i.v. dose in male cynomolgus monkeys (n=3). Dosing solutions were prepared by dissolving TRV0109101 in 10% ethanol and 10% cremophor and 80% sterile water. Monkeys received an i.v. dose of 3 mg/kg TRV0109101 via cephalic vein injection in a 1 mL/kg dose volume. Blood was collected into K2EDTA tubes predose and 0.083, 0.25, 0.5, 1, 2, 4, 8, 12 and 24 hr postdose from a cephalic or saphenous vein and processed to plasma.

Hot plate - Mouse and rat hot plate assays were adapted from (Tyers, 1980) and performed as previously described (Dewire et al., 2013). Animals were allowed to acclimate to the vivarium for 48 hour prior to assay. Animals were placed individually on a heated surface (56°C for mice, 52°C for rats) and the time interval between placement and a shaking, licking, or tucking of the hind paw was recorded as the baseline latency response. Post-drug latencies were recording 30 minutes after administration (s.c.) of vehicle (10:10:80), TRV0109101 or morphine with a maximal latency time set at 30 seconds. MPE was calculated as outlined in Methods.

Rat Tail-flick - The tail-flick assay was performed as previously described (Dewire et al., 2013). Male Sprague-Dawley rats (200–250 g) were allowed to acclimate to the vivarium for 48 hour prior to surgery. Briefly, animals were randomly assigned to vehicle (10:10:80), TRV0109101, or morphine treatment groups. Each animal was tested to determine the baseline response before drug treatment. Rats were gently restrained using a towel and the distal third of the tail was placed on the tail-flick apparatus (Columbus Instruments, Columbus, OH). Baseline temperature was set to a thermal stimulus that would produce a consistent baseline response of 3–6 seconds. The latency of the rat to withdraw the tail from the radiant thermal stimulus was recorded. At 30 minutes postdrug (s.c.,), animals were retested. A cutoff time of 15 seconds was used to prevent injury to the animal. MPE was calculated as described in materials and methods.

Rat incisional Pain - The incisional pain assay was performed as previously described (Dewire et al., 2013). Male Sprague-Dawley rats (200–250 g) were acclimated for 48 hour priosr to surgery. Twenty-four hours after surgery, animals were randomly assigned to vehicle (10:10:80), TRV0109101, or morphine treatment groups. All compounds were administered i.v. as a bolus in the rat tail (1 ml/kg). Tactile sensitivity (paw withdrawal threshold) for the injured hindpaw was assayed using von Frey filaments and the up/down method previously described [19; 28]. Mechanical allodynia was measured 30 minutes after drug administration.

Glass Bead Colonic Motility Assay - The glass bead colonic motility assay was performed as described in (Dewire et al., 2013)]. Mice (male C57BL/6J, 20–25 g) were fasted overnight and allowed free access to water the night before the experiment. Vehicle (10:10:80), TRV0109101, or morphine was administered 20 minutes before the insertion of a single 2-mm glass bead 2 cm into the distal colon of each mouse [39]. Time until bead expulsion was recorded. The assay was monitored with a maximum latency to expulsion of 240 minutes (100% MPE).

Fecal Boli Assay - The fecal boli assay was performed as previously described (Dewire et al., 2013). Mice (male C57BL/6J, 20–25 g) were allowed access to food and water ad libitum. Vehicle (10:10:80), TRV0109101, or morphine was administered (s.c.) 20 minutes after animals were placed individually in a testing chamber. Fecal boli were removed from each animal's test chamber and weighed hourly for 4 hours [39]. 100% MPE is defined in this assay as zero grams fecal boli production, and vehicle treated animals define the 0% effect boundary.

SUPPLEMENTAL TABLES (3) AND FIGURES (8)

TRV0109101, a G protein-biased agonist of the μ-opioid receptor, does not promote opioid-induced mechanical allodynia following chronic administration

Michael Koblish, Richard Carr III, Edward R. Siuda, David H. Rominger, William Gowen-MacDonald, Conrad L. Cowan, Aimee L. Crombie, Jonathan D. Violin, Michael W. Lark

Supplemental Table 1: TRV0109101 functional and selectivity analysis. Potency and efficacy for inhibition of cAMP production and increases in β-arrestin2 recruitment are reported as percent maximal response to morphine (MOPR), U-69,593 9 (KOPR), DPDPE (DOPR) or Nociceptin (NOPR).

TRV0109101	Inhibition of cAMP production			β-arrestin2 recruitment		
	pEC_{50}	S.E.	Efficacy (%)	pEC_{50}	S.E.	Efficacy (%)
hMOPR	-8.0	0.03	81	-7.2	0.16	23
hDOPR	-6.2	0.05	67	N.Q.	N.Q.	N.Q.
hKOPR	-5.8	0.05	60	N.Q.	N.Q.	N.Q.
hNOPR	-6.5	0.04	87	N.Q.	N.Q.	N.Q.
mMOPR	-9.0	0.08	84	-7.7	0.07	61
mDOPR	-5.8	0.06	62	N.Q.	N.Q.	N.Q.
mKOPR	-6.2	0.05	65	N.Q.	N.Q.	N.Q.

TRV0109101, a G protein-biased agonist of the μ-opioid receptor, does not promote opioid-induced mechanical allodynia following chronic administration

Michael Koblish, Richard Carr III, Edward R. Siuda, David H. Rominger, William Gowen-MacDonald, Conrad L. Cowan, Aimee L. Crombie, Jonathan D. Violin, Michael W. Lark

Supplemental Table 2: In vitro pharmacology: radioligand binding analysis. TRV0109101 (10 μM) binding specificity was analyzed by the CEREP ExpresSProfile against 55 representative GPCRs, ion channel and monoamine transporters.

Target of Interest	% Inhibition
A_1 (antagonist radioligand)	-8
A_{2A} (agonist radioligand)	13
A_3 (agonist radioligand)	-12
α_1 (non-selective) (antagonist radioligand)	9
α_2 (non-selective) (antagonist radioligand)	18
β_1 (agonist radioligand)	-13
β_2 (agonist radioligand)	8
AT_1 (antagonist radioligand)	-25
B_2 (agonist radioligand)	1
CB_1 (agonist radioligand)	6
CCR1 (agonist radioligand)	1
CXCR2 (IL-8B) (agonist radioligand)	-21
CCK1 (CCKA) (agonist radioligand)	-14
D_1 (antagonist radioligand)	9
D_{2S} (antagonist radioligand)	16
ETA (agonist radioligand)	-12
GAL_2 (agonist radioligand)	-6
H_1 (antagonist radioligand)	10
H_2 (antagonist radioligand)	-11
MC_4 (agonist radioligand)	4
MT_1 (ML) (agonist radioligand)	10
M_1 (antagonist radioligand)	-2
M_2 (antagonist radioligand)	5
M_3 (antagonist radioligand)	14
NK_2 (agonist radioligand)	4
NK_3 (antagonist radioligand)	13
Y_1 (agonist radioligand)	-24
Y_2 (agonist radioligand)	-8
NTS_1 (NT_1) (agonist radioligand)	-4
δ (DOP) (agonist radioligand)	66
κ (KOP) (agonist radioligand)	93
μ (MOP) (agonist radioligand)	100
NOP (ORL1) (agonist radioligand)	76
EP_4 (agonist radioligand)	2
5-HT_{1A} (agonist radioligand)	55
5-HT_{1B} (antagonist radioligand)	-5
5-$HT2_A$ (antagonist radioligand)	14
5-HT_{2B} (agonist radioligand)	8
5-HT_3 (agonist radioligand)	6
5-$HT5_a$ (agonist radioligand)	-5
5-HT_6 (agonist radioligand)	2
5-HT_7 (agonist radioligand)	-24
sst (non-selective) (agonist radioligand)	-12
$VPAC_1$ (VIP_1) (agonist radioligand)	-6
V_{1a} (agonist radioligand)	5
GABA (non-selective) (agonist radioligand)	9
Ca^{2+}(antagonist radioligand)	31
K_V (antagonist radioligand)	-6
SKC_a (antagonist radioligand)	-2
σ (non-selective) (agonist radioligand	71
BZD (central) (agonist radioligand)	-12
Cl^- channel (GABA-gated) (antagonist radioligand)	3
dopamine transporter (antagonist radioligand)	18
norepinephrine transporter (antagonist radioligand)	2
5-HT transporter (antagonist radioligand)	0

TRV0109101, a G protein-biased agonist of the μ-opioid receptor, does not promote opioid-induced mechanical allodynia following chronic administration

Michael Koblish, Richard Carr III, Edward R. Siuda, David H. Rominger, William Gowen-MacDonald, Conrad L. Cowan, Aimee L. Crombie, Jonathan D. Violin, Michael W. Lark

Supplemental Table 3: A summary of TRV0109101 pharmacokinetic parameters determined in mice, rats, dogs and cynomolgus monkeys by various routes of administration.

Pharmacokinetics of TRV0109101 in mouse and rat plasma

Species (route)	Dose (mg/kg)	AUC_{LAST} (hr•ng/mL)	Tmax (hr)	$T_{1/2}$ (hr)	Cmax (ng/mL)	%F
Mouse (s.c.)	10	1790	0.5	0.8	1560	77
Mouse (p.o.)	10	9	0.25	0.3	15	0.5
Rat (s.c.)	1	182	1	0.8	101	NC

Pharmacokinetics of TRV0109101 in plasma and brain following s.c. administration in mice

Sample	AUC_{LAST} (hr•ng/mL)	Tmax (hr)	$T_{1/2}$ (hr)	Cmax (ng/mL or ng/g)
Plasma	1790	0.5	0.8	1560
Brain	5550	0.5	0.9	5070

Pharmacokinetics of TRV0109101 (i.v.) in mouse, rat, dog, and cynomolgus monkey

Species	Dose (mg/kg)	AUC_{LAST} (hr•ng/mL)	terminal half-life $t_{1/2}$ (hr)	Clearance (L/kg/hr)	Vss (L/kg)
Mouse	3	696	0.9	4.3	2.9
Rat	3	769	0.9	3.9	2.8
Dog	1	1393	3.6	0.8	1.4
Monkey	0.3	315	4.7	0.9	2.4

Pharmacokinetics of TRV0109101 (i.v. infusion) in rat

Species	Dose (mg/kg/hr)	AUC_{LAST} (hr•ng/mL)	terminal half-life $t_{1/2}$ (hr)	Clearance (L/kg/hr)	Vss (L/kg)	Cmax (ng/mL)
Rat	2	2286	0.5	5.2	4.0	413
Rat	5	6827	0.4	4.4	1.8	1350

NC = not tested (no i.v. arm in this study)

AUC_{LAST}, area under the concentration curve from time = 0 to 8 hours (for rodent signle PK) and 24 hours (for dog and monkey)

V_{ss}, volume at steady-state

TRV0109101, a G protein-biased agonist of the μ-opioid receptor, does not promote opioid-induced mechanical allodynia following chronic administration

Michael Koblish, Richard Carr III, Edward R. Siuda, David H. Rominger, William Gowen-MacDonald, Conrad L. Cowan, Aimee L. Crombie, Jonathan D. Violin, Michael W. Lark

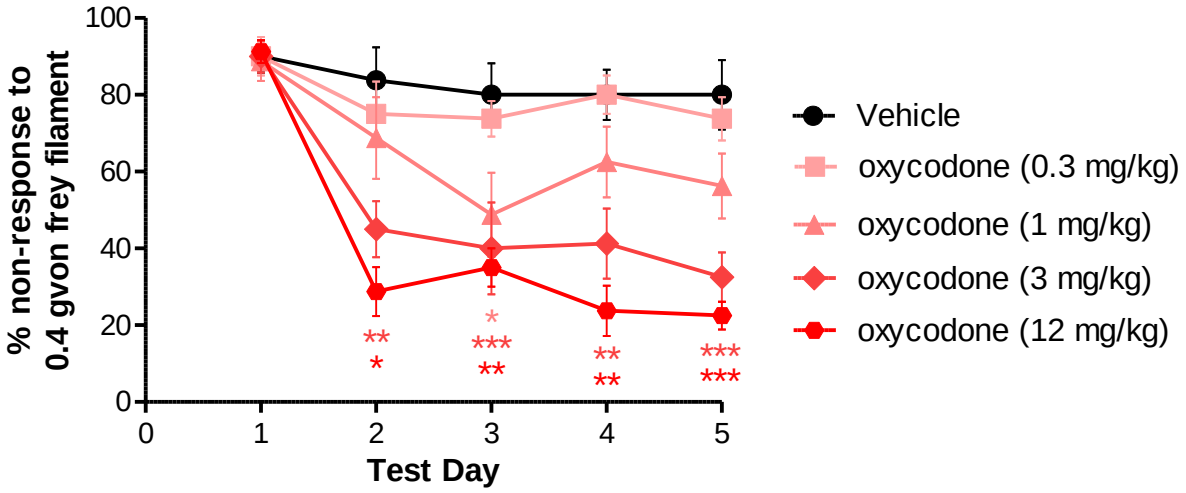

Figure S1: Repeated oxycodone administration produces opioid-induced mechanical allodynia in a dose-responsive manner. Mechanical allodynia was measured over 5 days in mice in response to twice daily (s.c.) vehicle (saline; n = 8), or oxycodone (0.3, 1, 3 and 12 mg/kg; n = 8). *** $p < 0.001$ via Two Way Repeated Measures ANOVA with Bonferroni post-tests to vehicle). Data are mean ± SEM (* $p < 0.05$, ** $p < 0.01$, *** $p < 0.001$ via Two Way Repeated Measures ANOVA with Bonferroni post-tests to vehicle).

TRV0109101, a G protein-biased agonist of the μ-opioid receptor, does not promote opioid-induced mechanical allodynia following chronic administration

Michael Koblish, Richard Carr III, Edward R. Siuda, David H. Rominger, William Gowen-MacDonald, Conrad L. Cowan, Aimee L. Crombie, Jonathan D. Violin, Michael W. Lark

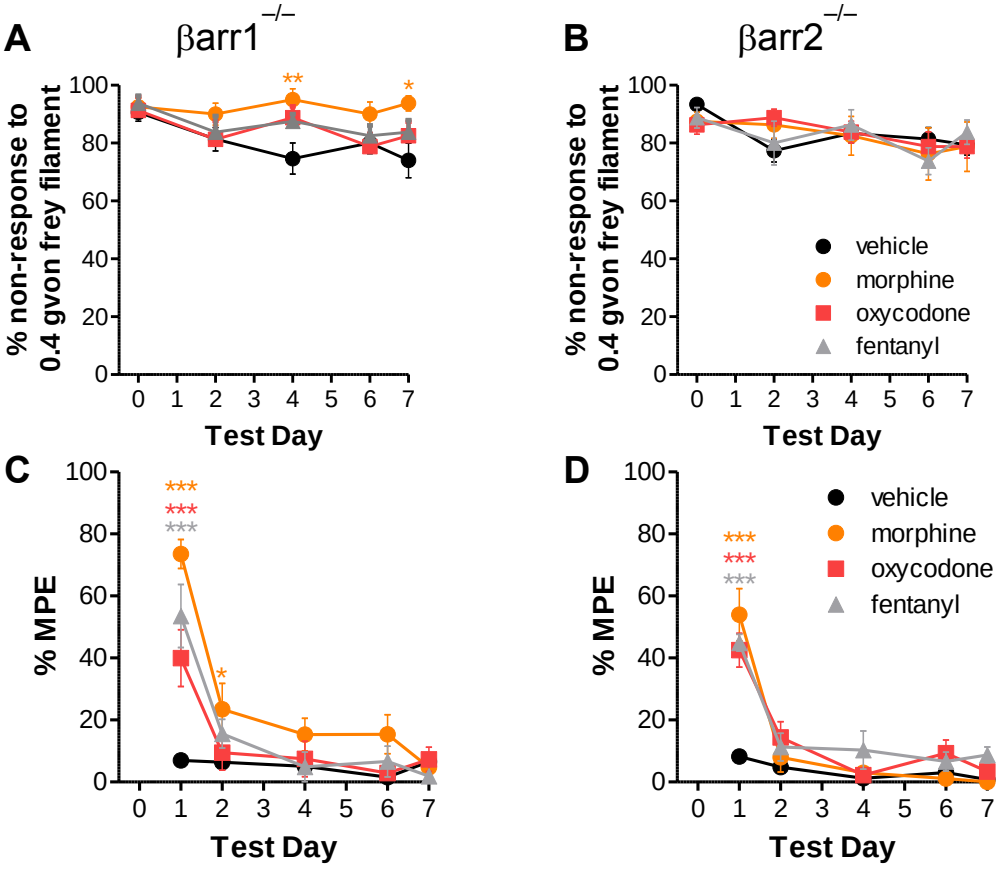

Figure S2: βarr1-KO and βarr2-KO mice do not exhibit opioid-induced mechanical allodynia but develop μ-opioid-induced tolerance to thermal stimuli. Mechanical allodynia was measured over 7 days in βarr1-KO **(A)** and βarr2-KO **(B)** mice in response to a chronic minipump infusion (7 days) with vehicle (saline, n=15), morphine (48 mg/kg/day, n = 8), oxycodone (25 mg/kg/day, n=8) or fentanyl (3.2 mg/kg/day, n = 8). 5 min after testing for mechanical allodynia, thermal (56°C) hot plate antinociceptive responses in βarr1-KO **(C)** and βarr2-KO **(D)** mice were measured. Data are mean ± SEM (* $p < 0.05$, ** $p < 0.01$, *** $p < 0.001$ via Two Way Repeated Measures ANOVA with Bonferroni post-tests to vehicle).

TRV0109101, a G protein-biased agonist of the μ-opioid receptor, does not promote opioid-induced mechanical allodynia following chronic administration

Michael Koblish, Richard Carr III, Edward R. Siuda, David H. Rominger, William Gowen-MacDonald, Conrad L. Cowan, Aimee L. Crombie, Jonathan D. Violin, Michael W. Lark

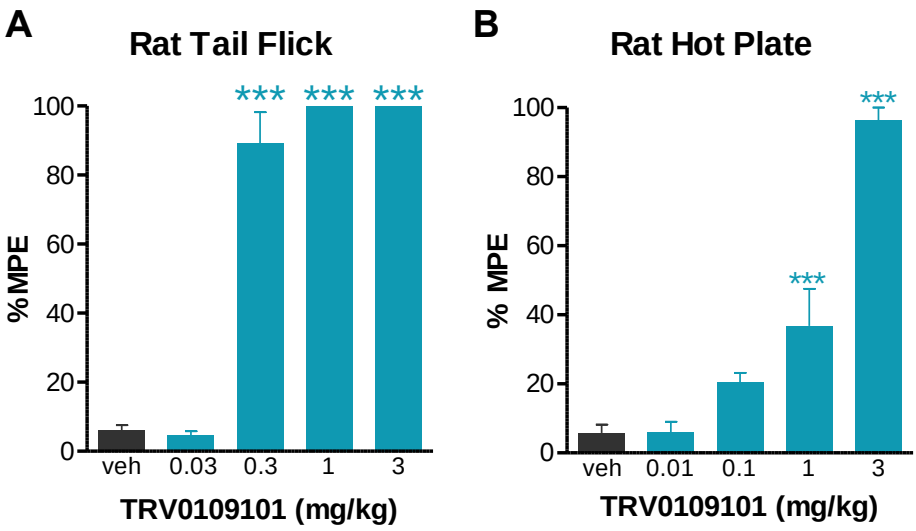

Figure S3: Analgesia produced by TRV0109101 in tail flick and hot plate assays. (A) Rat tail flick latencies were performed for TRV0109101. Percent of maximum possible response (15-second cutoff) is plotted. Rats were injected s.c. with either vehicle (grey bar; n = 6) or TRV0109101 (blue bars; n = 4-9/group). **(B)** Rats were injected s.c. with either vehicle (grey; n = 9) or TRV0109101 (blue; n = 8-11) at the indicated doses and 30 minutes later subjected to a 52°C hot plate assay. The % MPE was based on a 30-second assay cutoff.

TRV0109101, a G protein-biased agonist of the μ-opioid receptor, does not promote opioid-induced mechanical allodynia following chronic administration

Michael Koblish, Richard Carr III, Edward R. Siuda, David H. Rominger, William Gowen-MacDonald, Conrad L. Cowan, Aimee L. Crombie, Jonathan D. Violin, Michael W. Lark

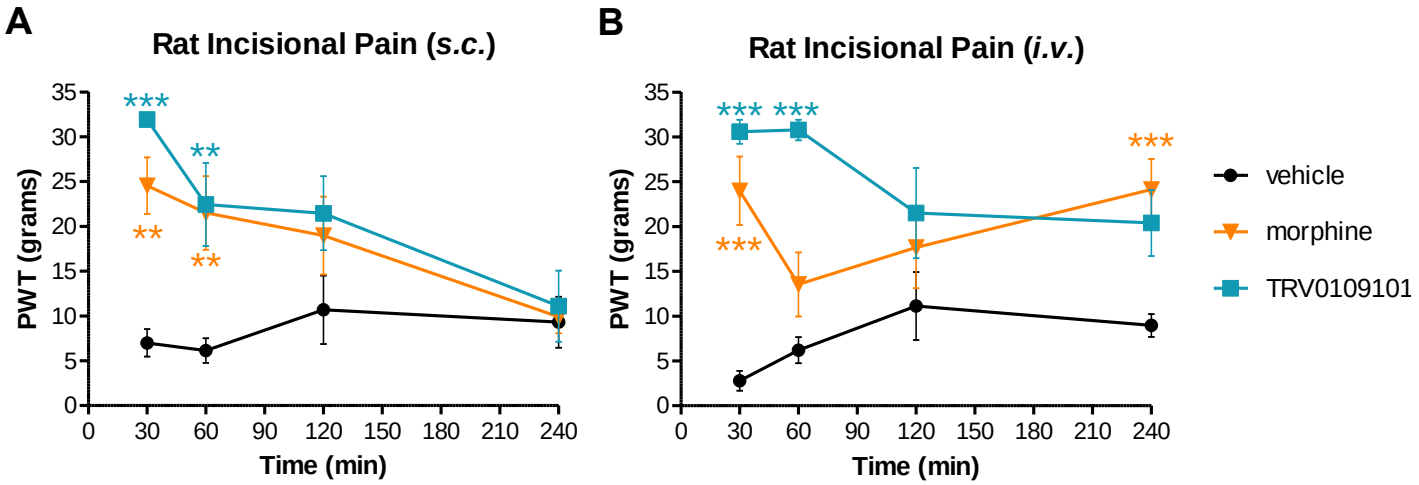

Figure S4: Analgesia produced by morphine and TRV0109101 in rat incisional pain assay. (A) Subcutaneous (s.c.) administration of TRV0109101 (1 mg/kg; blue; n = 8) and morphine (3 mg/kg; orange; n = 8) are active in the rat hindpaw incisional pain model compared to vehicle controls (black, n = 7). **(B)** Intravenous (i.v.) administration of TRV0109101 (1 mg/kg; blue; n = 7) and morphine (3 mg/kg; orange; n = 8) are active in rat incisional pain model compared to vehicle controls (black; n = 8). Paw withdrawal threshold is plotted on the Y axis. Data are mean ± SEM (** $p < 0.01$, *** $p < 0.001$ via Two Way Repeated Measures ANOVA with Bonferroni post-tests to vehicle).

TRV0109101, a G protein-biased agonist of the μ-opioid receptor, does not promote opioid-induced mechanical allodynia following chronic administration

Michael Koblish, Richard Carr III, Edward R. Siuda, David H. Rominger, William Gowen-MacDonald, Conrad L. Cowan, Aimee L. Crombie, Jonathan D. Violin, Michael W. Lark

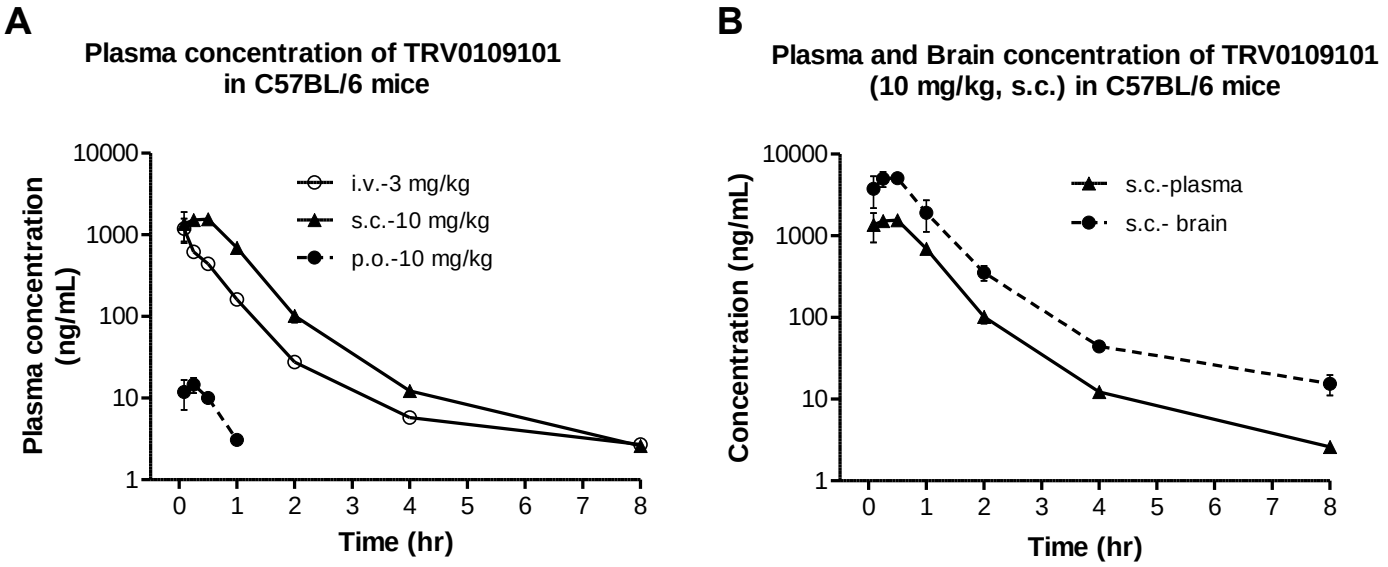

Figure S5: TRV0109101 in vivo pharmacokinetics. (A) Time course of TRV0109101 plasma concentration following i.v. (3 mg/kg), s.c. (10 mg/kg) and p.o. (10 mg/kg) dosing in mice (n = 3 animals/time point). **(B)** Time course of TRV0109101 plasma and brain concentrations following s.c. (10 mg/kg) dose in mice (n = 3 animals/time point).

TRV0109101, a G protein-biased agonist of the μ-opioid receptor, does not promote opioid-induced mechanical allodynia following chronic administration

Michael Koblish, Richard Carr III, Edward R. Siuda, David H. Rominger, William Gowen-MacDonald, Conrad L. Cowan, Aimee L. Crombie, Jonathan D. Violin, Michael W. Lark

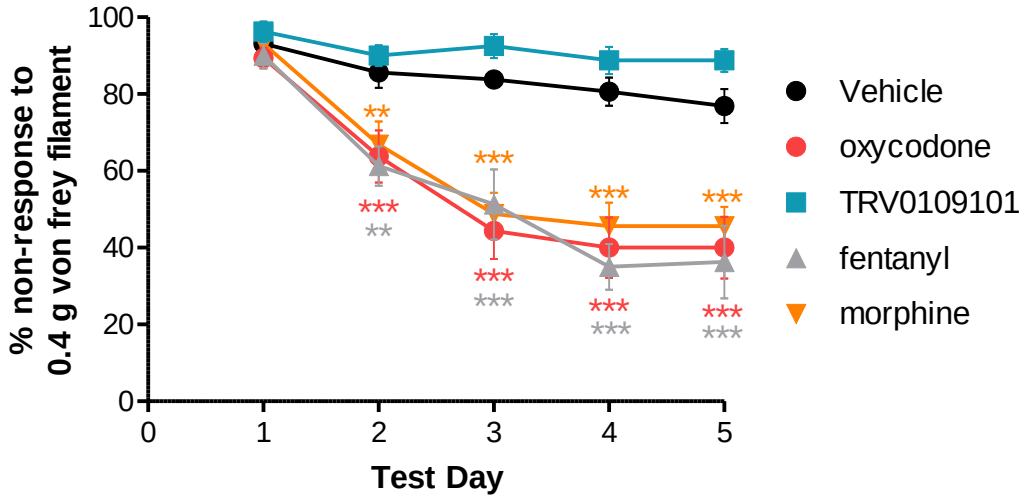

Figure S6: Repeated TRV0109101 administration does not produce opioid-induced mechanical allodynia. Mechanical allodynia was measured over 5 days in mice in response to twice daily (s.c.) vehicle (saline or 10:10:80; n = 16), morphine (day 1-3: 20 mg/kg; day 4: 40 mg/kg; n = 16), oxycodone (day 1-3: 12 mg/kg; day 4: 24 mg/kg; n = 16), fentanyl (day 1-3: 0.6 mg/kg; day 4: 1.2 mg/kg; n = 16), or TRV0109101 (day 1-3: 20 mg/kg; day 4: 40 mg/kg; n = 8). Data are mean ± SEM (** $p < 0.01$, *** $p < 0.001$ via Two Way Repeated Measures ANOVA with Bonferroni post-tests to vehicle).

TRV0109101, a G protein-biased agonist of the μ-opioid receptor, does not promote opioid-induced mechanical allodynia following chronic administration

Michael Koblish, Richard Carr III, Edward R. Siuda, David H. Rominger, William Gowen-MacDonald, Conrad L. Cowan, Aimee L. Crombie, Jonathan D. Violin, Michael W. Lark

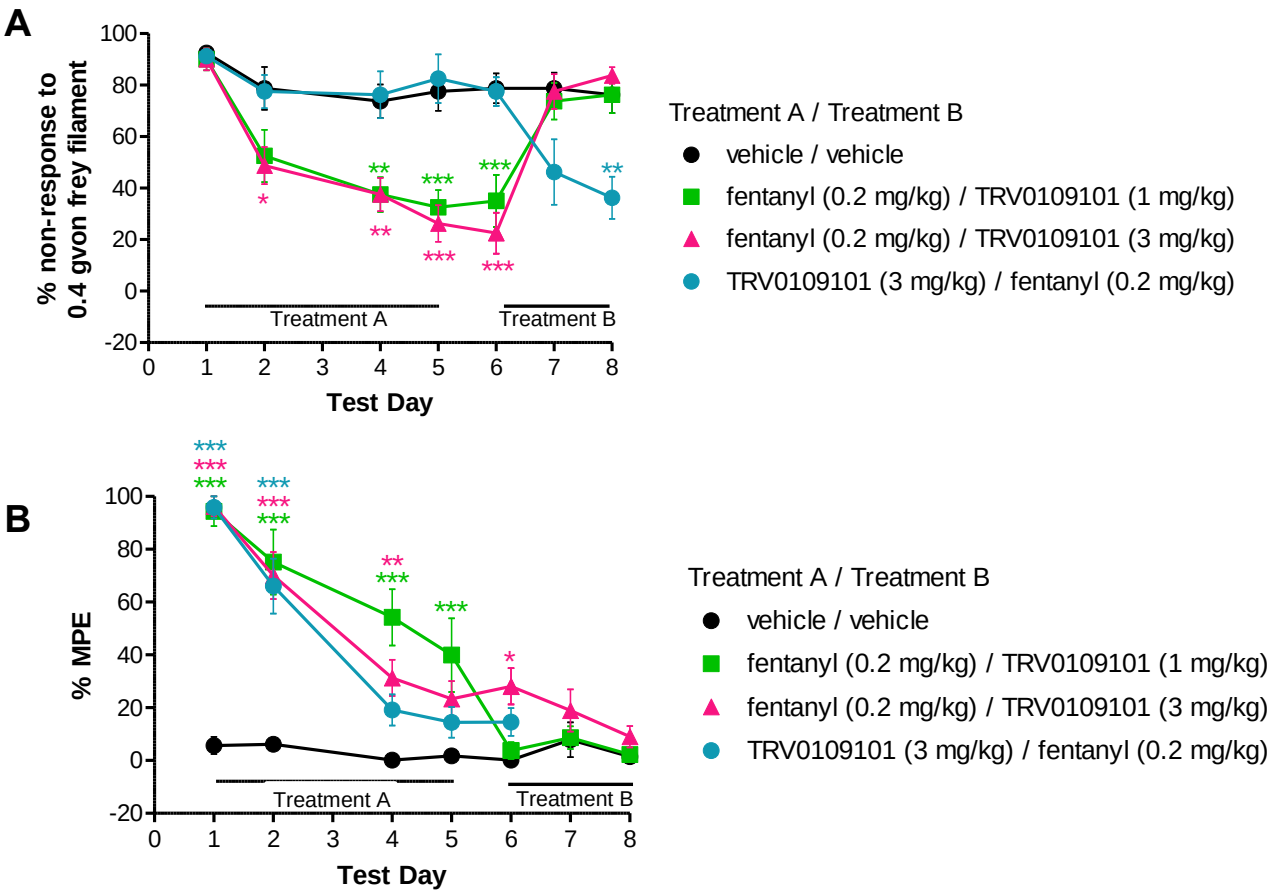

Figure S7: Repeated fentanyl administration-induced mechanical allodynia is reversed by TRV0109101. (A) Treatment A - Mice were dosed twice daily (s.c.) with saline, fentanyl (day 1-5: 0.2 mg/kg), or TRV0109101 (day 1-5: 3 mg/kg). Treatment B – After von frey testing on day 6, fentanyl treated mice were switched to twice daily (s.c.) TRV0109101 (n = 8, 1 mg/kg) or TRV0109101 (n = 8, 3 mg/kg) through day 8. TRV0109101 treated mice were switched to twice daily (s.c.) fentanyl (n = 8, 0.2 mg/kg). **(B)** 5 minutes after dosing, thermal (56°C) hot plate antinociceptive responses were measured. Data are mean ± SEM (* $p < 0.05$, ** $p < 0.01$, *** $p < 0.001$ via Two Way Repeated Measures ANOVA with Bonferroni post-tests to vehicle).

TRV0109101, a G protein-biased agonist of the μ-opioid receptor, does not promote opioid-induced mechanical allodynia following chronic administration

Michael Koblish, Richard Carr III, Edward R. Siuda, David H. Rominger, William Gowen-MacDonald, Conrad L. Cowan, Aimee L. Crombie, Jonathan D. Violin, Michael W. Lark

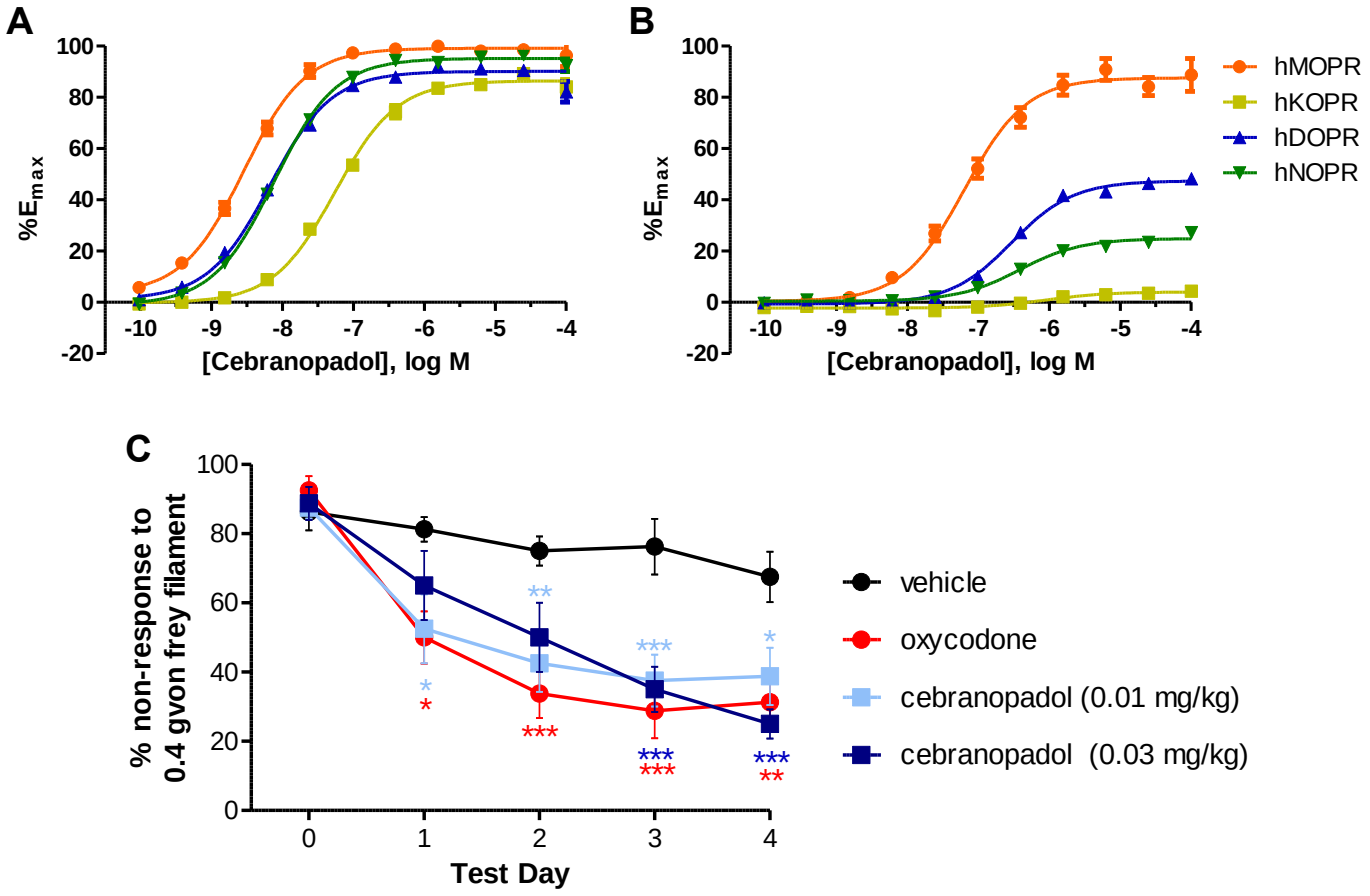

Figure S8: Cebranopadol inhibits cAMP accumulation and promotes β-arrestin recruitment *in vitro*, while repeated administration results in opioid-induced mechanical allodynia *in vivo*. Cebranopadol dose dependently inhibits cAMP accumulation across all opioid receptor expressing cell lines **(A)** with varying degrees of activity in β-arrestin recruitment **(B)** [MOPR (orange), KOPR (yellow), DOPR (blue) and NOPR (green). Data are mean ± SEM for at least 3 independent experiments. **(C)** Mechanical allodynia was measured over 5 days in mice in response to twice daily (s.c) vehicle (saline or 10:10:80; n = 8), oxycodone (day 1-3: 12 mg/kg; day 4: 24 mg/kg; n = 8), or cebranopadol (day 1-4: 0.01 or 0.03 mg/kg; n = 8). Data are mean ± SEM (* $p < 0.05$, ** $p < 0.01$, *** $p < 0.001$ via Two Way Repeated Measures ANOVA with Bonferroni post-tests to vehicle).